CANADIAN THESES ON MICROFICHE

I.S.B.N.

THESES CANADIENNES SUR MICROFICHE

National Library of Canada
Collections Development Branch

Canadian Theses on
Microfiche Service

Ottawa, Canada
K1A 0N4

Bibliothèque nationale du Canada
Direction du développement des collections

Service des thèses canadiennes
sur microfiche

NOTICE

The quality of this microfiche is heavily dependent upon the quality of the original thesis submitted for microfilming. Every effort has been made to ensure the highest quality of reproduction possible.

If pages are missing, contact the university which granted the degree.

Some pages may have indistinct print especially if the original pages were typed with a poor typewriter ribbon or if the university sent us a poor photocopy.

Previously copyrighted materials (journal articles, published tests, etc.) are not filmed.

Reproduction in full or in part of this film is governed by the Canadian Copyright Act, R.S.C. 1970, c. C-30. Please read the authorization forms which accompany this thesis.

THIS DISSERTATION
HAS BEEN MICROFILMED
EXACTLY AS RECEIVED

AVIS

La qualité de cette microfiche dépend grandement de la qualité de la thèse soumise au microfilmage. Nous avons tout fait pour assurer une qualité supérieure de reproduction.

S'il manque des pages, veuillez communiquer avec l'université qui a conféré le grade.

La qualité d'impression de certaines pages peut laisser à désirer, surtout si les pages originales ont été dactylographiées à l'aide d'un ruban usé ou si l'université nous a fait parvenir une photocopie de mauvaise qualité.

Les documents qui font déjà l'objet d'un droit d'auteur (articles de revue, examens publiés, etc.) ne sont pas microfilmés.

La reproduction, même partielle, de ce microfilm est soumise à la Loi canadienne sur le droit d'auteur, SRC 1970, c. C-30. Veuillez prendre connaissance des formules d'autorisation qui accompagnent cette thèse.

LA THÈSE A ÉTÉ
MICROFILMÉE TELLE QUE
NOUS L'AVONS REÇUE

NL-339 (r. 82/08)

Canada

National Library of Canada
Bibliothèque nationale du Canada

Canadian Theses Division
Division des thèses canadiennes

Ottawa, Canada
K1A 0N4

PERMISSION TO MICROFILM — AUTORISATION DE MICROFILMER

• Please print or type — Écrire en lettres moulées ou dactylographier

Full Name of Author — Nom complet de l'auteur

RAHMAN, Fazal-Ur

Date of Birth — Date de naissance	Country of Birth — Lieu de naissance
September 2, 1953.	PAKISTAN

Permanent Address — Résidence fixe

c/o Department of Physics
University of Ottawa

Title of Thesis — Titre de la thèse

SINGLE AND DOUBLE ELECTRON DETACHMENT CROSS SECTIONS OF F^-, Cl^- AND I^- IN RARE GASES

University — Université

UNIVERSITY OF OTTAWA

Degree for which thesis was presented — Grade pour lequel cette thèse fut présentée

Ph.D.(Physics)

Year this degree conferred — Année d'obtention de ce grade	Name of Supervisor — Nom du directeur de thèse
1984	Dr. Brian Hird

Date	Signature
October 11, 1984.	Fazal-ur Rahman

Single and double electron detachment cross sections of F^-, Cl^- and I^- in rare gases

by

Fazal-ur-Rahman

A thesis submitted to the School of Graduate Studies and Research of the University of Ottawa in partial fulfilment of the requirements for the degree of Doctor of Philosophy in Physics.

Department of Physics
Faculty of Science and Engineering
University of Ottawa
Ottawa, Canada

1984.

UNIVERSITÉ D'OTTAWA / UNIVERSITY OF OTTAWA
École des études supérieures/School of Graduate Studies
et de la recherche and Research

NAME OF AUTHOR RAHMAN, Fazal-Ur

TITLE OF THESIS SINGLE AND DOUBLE ELECTRON DETACHMENT CROSS SECTIONS OF F^-, Cl^- AND I^- IN RARE GASES

DEGREE Ph.D. (Physics) YEAR GRANTED 1984

Fazal-ur-Rahman
(Signed) (Author)

Date: October 11, 1984.

Permanent Address:
c/o Department of Physics
University of Ottawa

UNIVERSITÉ D'OTTAWA
UNIVERSITY OF OTTAWA

UNIVERSITÉ D'OTTAWA / UNIVERSITY OF OTTAWA
École des études supérieures/School of Graduate Studies

Title of thesis SINGLE AND DOUBLE ELECTRON DETACHMENT CROSS SECTIONS OF F^-, Cl^- AND I^- IN RARE GASES

Name of candidate RAHMAN, Fazal-ur

Degree Ph.D. Department PHYSICS

Date of defence October 11, 1984.

This thesis prepared under the supervision of B. Hird has been approved by a jury composed of the following examiners:

J. ARMITAGE
P. BERNARD
R.L. CHAMPION
J. HEBERT

(Dean of Graduate Studies)

ABSTRACT

The single electron detachment cross section σ_{-0} and two electrons loss cross section σ_{-+} from negative ions of F^-, Cl^- and I^- in a single collision with rare gas atoms were measured between 10 keV and 125 keV energy range. The initial growth method was used with a thin target to calculate the cross sections. The σ_{-0} cross section is found to be almost energy independent for F^- and Cl^- in He and Ne and for I^- in He only, but are found to increase with energy in heavy targets.

A good theoretical fit, using a zero radius potential formulation for the single electron detachment cross section has been obtained for the Cl^- + Ar system up to 90 keV energy, beyond which disagreement was found . The predictions of the complex potential model for the Cl^- + Rg system show an increasing cross section with energy from threshold to some few hundreds of eV, after which it decreases for all rare gas targets throughout our energy range.

The σ_{-+} cross section is found to have its largest magnitude for F^- and Cl^- in lighter rare gas targets, whereas for I^- it is found to depend on target atomic number. A close similarity between the σ_{-+} and the σ_{0+} cross sections suggests that two electron detachment is a sequental process in which one electron is detached first and then a second electron is removed at a smaller interaction radius.

ACKNOWLEDGEMENTS

My sincere thanks are to my research supervisor Dr.Brian Hird whose constant guidance and patience during the research, made it possible for me to complete this work sucessfully. I also wish to thank Dr.Brian, A.Logan for his valuable technical help received from time to time and to Dr.C.Benson for his general guidance. My sincere gratitude is also due to Mr. C.N.Goodchild and all his staff and to Mr.Art Buser for the construction and electronics work involved in this research.

I am grateful to my brother Mr.F.Karim Khan for looking after my and our family interests carefully during my absence from home.

Finally I am thankful to the Government of Pakistan to provide me the opportunity in the form of COT scholarship to complete this work.

C O N T E N T S

List of figures

LIST OF TABLES

CHAPTER 1

INTRODUCTION

1.1 HISTORICAL BACKGROUND.

Beside spectroscopic studies, another powerful tool to investigate the atomic structure is scattering, where the beam of particles is made to scatter from the target particles and measurements of scattering angles, energy losses and atomic cross sections provide useful information about the atom. Among possible scattering events, charge exchange processes are important because of their leading role in Astrophysics, Plasma Physics, the design of heavy ions accelerators and more recently in Laser Physics. Much work has been done on charge exchange processes involving positive ions. However similar work on negative ions was started in 1952 by Hasted[1], who measured the electron detachment cross sections from negative ions in negative ion-atom collisions.

Negative ions posess very interesting properties but prior to 1935 there were not much information available. Massey's monograph[2] on negative ions published in 1937 was the first attempt to compile all the information available at that time. The publication of this monograph helped to stimulate research on negative ions. Many properties of negative ions such as electron binding energies, recombination, photoionization

etc., were discussed in detail in this monograph. Other important publications on negative ions are, the review article by Popp[3] and a recently published monograph by Smirnov[4].

Electron detachment from a negative ion when it collides with an atom is an important process which has been under intensive investigations for last three decades. Both Hasted in England and Bydin and Dukelskii[5] in 1955 in U.S.S.R made the first measurements of electron detachment cross sections at low energies. Many review articles have been published, of which the most important are by Allison[6], which gives the details of electron detachment cross section measurements involving hydrogen negative ions and by Risley[7], which reviews the work up to 1978 for almost every kind of atomic negative ion detachment cross section measurement. Some theoretical work has also been reviewed in Smirnovs monograph on negative ions.

1.2 GENERAL CONSIDERATIONS

A single collision between a negative ion and an atom may result in the production of a neutral atom, positive ion or a molecule. Considering the collision partners in their ground states, the following processes can be expected as a result of a collision between a negative ion A^- and a neutral atom B,

1. $A^- + B \longrightarrow A + B + e$
2. $A^- + B \longrightarrow A^+ + B + 2e$
3. $A^- + B \longrightarrow A + B^-$
4. $A^- + B \longrightarrow AB + e$

These processes are identified in order as a single electron detachment, double electron detachment, charge exchange, and the associative detachment of the electron which leads to the formation of a molecule. In the present measurements the target atoms involved were all rare gases which have the highest ionization potentials and no excited states of comparable energy to the valence electron binding energies in the incident negative ions. This indicates that the electron detachment process is the dominant one among the others. It is also relevant to mention that the electron transfer process which dominates most positive ions charge changing cross sections is probably not important even for target atoms which have stable negative ions, and can not occur otherwise. However a negative ion may be formed by charge transfer to an intermediate state, which then decays by electron emission after the ion and atom have separated. At kinetic energies up to about 1 keV, it has been possible to distinguish between simple detachment and the formation of an intermediate state by using energy loss spectroscopy on the fast ions and atoms from the collision[8].

Several measurements have been reported in which the electron detachment cross section σ_{-0} for halogen negative ions on

rare gas atoms has been studied thorougly with beam energies from the electron affinity to a few keV energy[1,5,9,10]. Generally two different approaches have been used to explain the electron detachment mechanism. Both of these models are based on the quasi- molecular description of the collision which assumes that the particle velocities are much less than the velocity of electrons in their classical Bohr orbits. The idea of Demkov[11] that the detachment can be described in terms of transformation of an incident discrete state into a virtual state, was used by Devdariani[12] to develop the so called zero radius potential (ZRP) theory and was tested successfully by Bydin et al[13] for negative halogen ion-rare gas collisions in an energy range of 100 eV to 1.4 keV . On the other hand the complex potential model describing the detachment process as a consequence of the decay of a quasi-stationary state, was used quite sucessfully by Champion and Doverspike[9] and Smith et al[10] to fit their electron detachment cross section measurements for halogen negative ions with rare gas atoms in the energy range from a few eV to about 200 eV.

The two electron detachment from a negative ion during its collision with a neutral atom was first identified by Dukelskii and Fedorenko[14]. They measured the σ_{-+} cross section for I^- ions in argon and nitrogen targets in the energy range 5 keV to 17.5 keV . They found a rapid increase in the σ_{-+} cross section with energy. Matic and Cobic[15] found that the σ_{-+} cross section

always increased with energy for C^- and O^- ions in rare gas targets in the 4 keV to 32 keV energy range. The collisional loss of two electrons from negative ions has not been studied theoretically.

The work presented in this thesis concerns single (σ_{-0}) and double electron detachment (σ_{-+}) cross section measurements for negative ions of fluorine[16,17], chlorine[18,19] and iodine[20] incident on rare gases in the energy range from 10 keV to 125 keV. The σ_{-0} cross section is found to be almost energy independent in He and Ne targets but increases with energy for heavier targets throughout our energy range. The self consistent field energies V(r) for the Cl^- + Ar system[21] were used in the Devdariani model[12] with a modification made by Gauyacq[22,23] to fit the present measurements. The agreement was quite good up to 90 keV energy beyond which the theory predicts a constant value, contrary to our measurements. As far as the σ_{-+} cross section is concerned it is found that F^- and Cl^- ions incident on rare gases, have larger magnitudes in lighter targets than in heavier targets. Somewhat similar behaviour was observed by Matic and Cobic[15] for O^- on rare gases. However for I^- on rare gases, the σ_{-+} cross section is found to depend on the target atomic number. No data has previously been reported on σ_{-0} and σ_{-+} cross section measurements in the 10 keV to 125 keV energy range for halogen negative ions incident on rare gases with the exception of Lichtenberg et al[24] who measured σ_{tot} and σ_{-+} for I^- incident

on He and Ar targets in the 20 keV to 220 keV energy range.

A review of the theoretical work is outlined in chapter 2. Chapter 3 describes the experimental technique and the measurement procedure, whereas chapter 4 is a discussion of the experimental data, together with a qualitative theoretical fit. The final conclusions are drawn in chapter 5.

CHAPTER 2

THEORETICAL ASPECTS OF NEGATIVE ION DETACHMENT

2.1 MOLECULAR ORBITAL DESCRIPTION OF THE COLLISION AND POTENTIAL CURVES.

In slow collisions, where the particle velocities are smaller than the classical orbital velocities, collisions can be treated within the frame-work of the Born Oppenheimer approximation of separating the nuclear and electronic motions and dealing with them independently. In ionization and excitation collisions among the two atomic particles, a diatomic molecule (quasi molecule) is temporarily formed. Thus in order to get a better understanding of these collisions, a molecular orbital treatment is more appropriate. The two body approximation becomes less satisfactory, except in the other extreme of very high energy collisions.

Consider an ion A^- and a neutral atom B at a fixed distance R apart. The allowed energies for the total system, which we may refer to as the molecule $(A + B)^-$, can be calculated by the usual quantum mechanical methods. This is done at each internuclear separation R. As $R \rightarrow \infty$, the total internal energy of the system will be equal to $U(\infty) = E_1(A^-) + E_1(B)$, where $E_1(A^-)$ and $E_1(B)$ are the energies of the ground states of the isolated particles A^- and B.[3] Now if the two particles start approaching

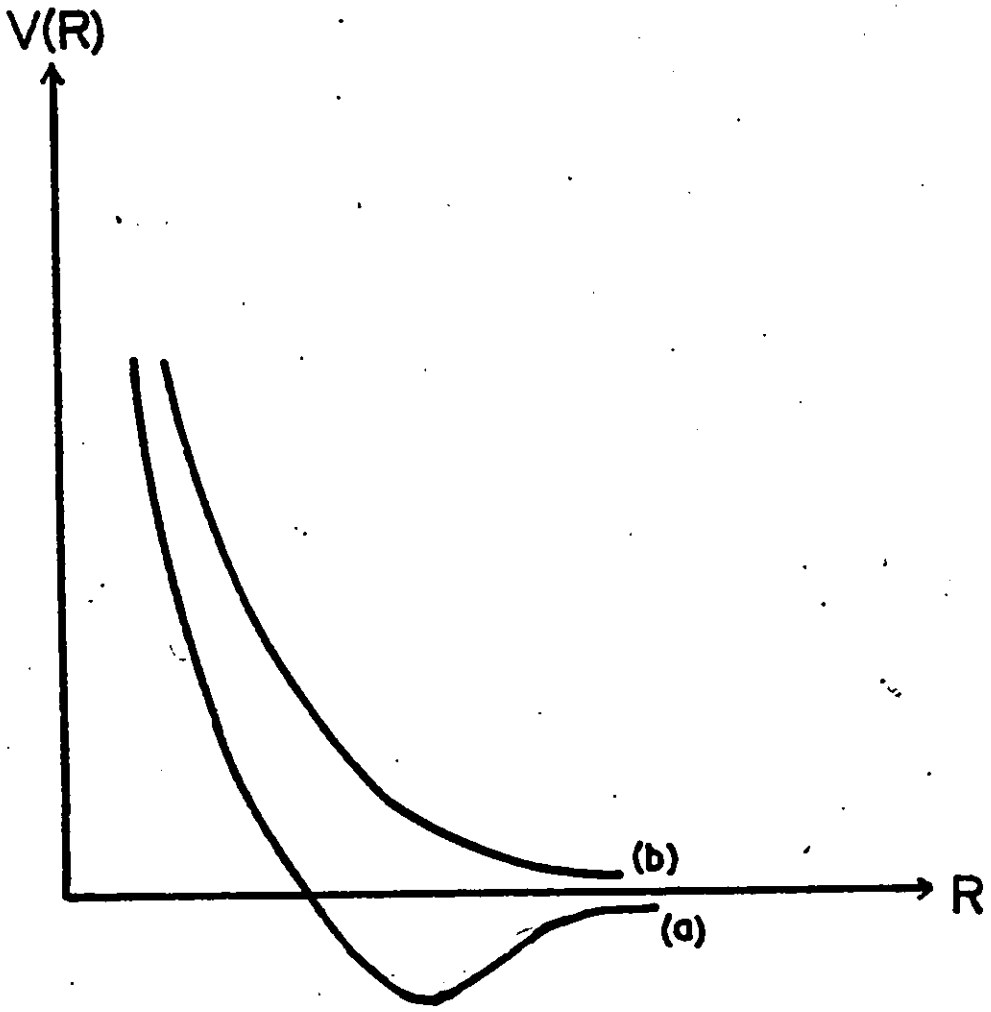

Fig.2.1:- Potential energy curves for two approaching particles,
(a) For stable molecule formation.
(b) For unstable molecule formation.

each other slowly, then the electronic energy takes up the value corresponding to the instantaneous position of the atoms. Thus in order to change the position of the atoms, not only the work must be done against the mutual interaction of the nuclei but also work must be supplied for the necessary change of electronic energy. The sum of electronic energy and the mutual interaction energy of the atoms acts as the potential energy of the system. The curves representing the variation of the effective potential energy of the atoms are referred to as potential curves. In fig. 2.1 two such potential curves are shown. For small internuclear separations, the total energy of the system has the form (a) or (b) of fig. 2.1. The curve (a) represents the potential energy of a system where a stable molecule is formed whereas curve (b) corresponds to an unstable molecular state.

2.2 ELECTRON DETACHMENT THEORIES.

The merging of a discrete energy level of a quasi molecule with the continuum of energies in negative ion-atom collisions is thought to be responsible for the detachment of electron from a negative ion. Various models and theories, in spite of their different approaches, are generally based on a curve crossing mechanism. This is a crossing of a discrete state with an infinite number of energy states so that the Landau-Zener two state formalism, which holds good in those cases where only

two discrete states intersect, is not appropriate. A review of the electron detachment theories will be given in the following pages.

2.3 EARLY WORK.

The very first experimental work of Hasted[1] on electron detachment cross section measurements was interpreted in terms of Masseys adiabatic criterion. According to this criterion for slow collisions, transitions from one state to another are possible only, when the collision time and the transition time are comparable. This criterion is a statement of the Heisenberg uncertainty principle as applied to atomic collisions. If $\Delta t = \frac{a}{v}$ is the time of interaction of the atoms, where a is an arbitrary interaction distance and v is the relative velocity of the colliding atoms, then in this time, the internal (electronic) energy is defined only to within $\Delta\epsilon \sim \frac{1}{\Delta t}$. Transitions to states having energies within this range of energy of the initial state may occur with a high probability, but the transitions to other states will be unlikely. Thus from the above one gets a condition, according to which transitions are improbable unless

$$\frac{a\,\Delta\epsilon}{v} \ll 1$$

Here $\Delta\epsilon$ is the separation between the energy states. Hasted[1] used asymptotic atomic energies to calculate $\Delta\epsilon$. Although he

successfully accounted for a number of observations this way, such a usage is not always appropriate, because the energies of electronic states can change substantially with internuclear distance, and two states that have quite different energies at infinite separations may become degenerate at finite R.

The first theoretical model specifically for electron detachment was proposed by Bydin and Dukelskii[5] and independently by Mason and Vanderslice[25]. It is based on the postulate that the potential energy curves of the colliding system $(A^- + B)$ and $(A+B)$ cross or come close to each other at some internuclear distance R_o. When the distance of closest approach R_{min} is less than R_o, the probablity of detachment is assumed to be unity and when R_{min} is greater than R_o it is assumed to be zero. From the conservation of energy at the distance of closest approach, where the radial component of velocity is zero, we can write for the kinetic energy of relative motion

$$\frac{1}{2}\frac{L^2}{MR_{min}^2} + V(R_{min}) = \frac{1}{2}Mv^2 \qquad (2.1)$$

Where M is the reduced mass of the system, v is the initial velocity of relative motion and L is the angular momentum of the particle at R_{min}. Rearrangment of above equation gives,

$$M^2v^2\left[1 - \frac{V(R_{min})}{E}\right] = \frac{L^2}{R_{min}^2}.$$

but

$$L = Mvb$$

Where b is the impact parameter. From the last two equations we get

$$b = R_{min}\left[1 - \frac{V(R_{min})}{E}\right]^{1/2} \qquad (2.2)$$

The electron detachment cross section is obtained from

$$\sigma_{DET} = \int_0^{R_0} 2\pi b\, db = \pi b^2 \Big|_0^{R_0}$$

$$\sigma_{DET} = \pi R_0^2\left[1 - \frac{V(R_0)}{E}\right] \qquad (2.3)$$

Where $V(R_o)$ is the common potential energy at $R = R_o$, E is the kinetic energy of the particles in the center of mass system and is related to the laboratory energy by

$$E = \frac{M_2}{M_1 + M_2} E_L \qquad (2.4)$$

where M_1 is the mass of the projectile particle and M_2 is that of target particle. Bydin and Dukelskii[5] assumed that R_o and $V(R_o)$ were variable parameters and obtained a good fit to their experimental data from 150 eV to about 2 keV center of mass energies. This formula ceases to valid when the center of mass collision energy E, approaches the repulsive interaction energy

$V(R_o)$ between the two particles at internuclear distance R_o. At the other extreme the formula gives poor agreement for energies, $E >> V(R_o)$, where the theoretical σ_{DET} cross section is constant, contrary to experiments. In the low energy region the nonvalidity of equation (2.3) is due to the importance of sub-barrier effects near threshold which are not taken into account. For higher energies the constant value of the cross section obtained from equation (2.3) is due to the unrealistic assumption that the detachment probability is unity for $R_{min} < R_o$ and zero for $R_{min} > R_o$. In fact significant detachment does take place for $R_{min} > R_o$ and the particles may not spend enough time with $R < R_o$ for complete detachment.

2.4 COMPLEX POTENTIAL MODEL.

The complex potential treatment[9,26] of the electron detachment process from a negative ion is applicable to slow collisions so that the formalism lies within the framework of a molecular orbital description of the collision. At infinite internuclear separations the potential energy curve of the (A^-+B) system lies below the corresponding curve of the (A+B+e) system by an amount equal to the electron affinity of the negative ion. The decrease in internuclear distance results in raising the energy of bound state of the system (A^-+B) relative to the (A+B+e) system, until at some internuclear separation R_o they

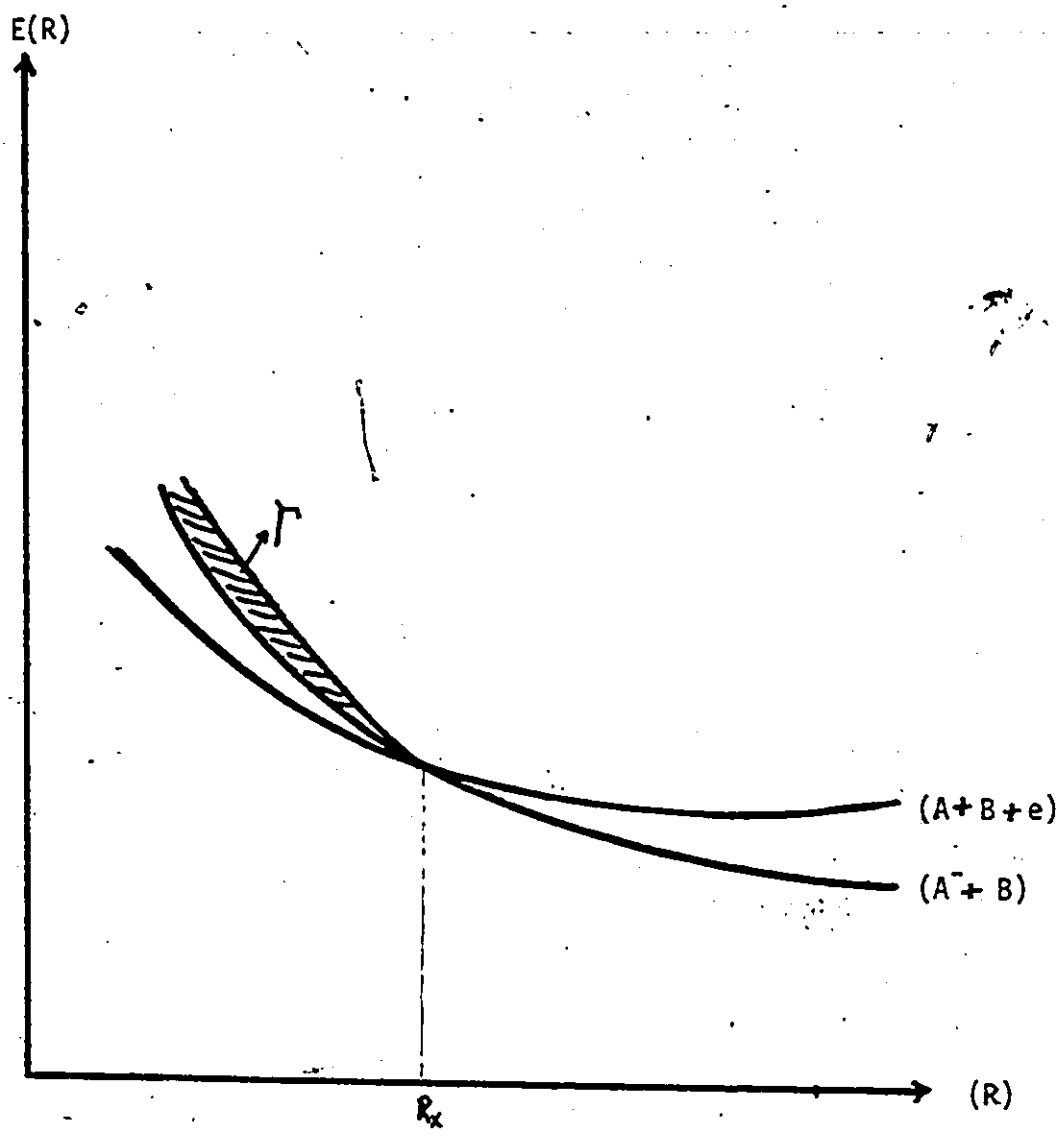

Fig.2.2:- The crossing of a bound $(A^- + B)$ state with the continuum of $(A+B+e)$ states. Γ is the width acquired after the crossing point.

become degenerate. At still smaller separations, the curve of the $(A^- + B)$ system lies in the continuum of curves of the (A+B+e) system (fig.2.2). Lam et al[26] have used a complex potential to describe the quasibound positive energy state, where $\Gamma(R)$ has the significance of the width for the decay to a free electron with kinetic energy E,

$$E = V(R) - \frac{1}{2}\Gamma(R) \qquad (2.5)$$

In the absence of detachment $\Gamma(R)$ is zero and the real part of the potential, V(R) determines the elastic scattering cross section. The survival probability of negative ion is by definition the solution of the equation,

$$\frac{dP_s}{dt} = -\Gamma P_s$$

Which gives

$$P_s = e^{-\int_{-\infty}^{+\infty} \Gamma\, dt} = e^{-2\int_{R_0}^{\infty} \Gamma(R)\, \frac{dR}{v_R}} \qquad (2.6)$$

Where R_o is the classical turning point and v_R, the radial velocity, is given by

$$v_R = v_\infty \left[1 - \frac{V(R)}{E} - \frac{b^2}{R^2}\right]^{1/2} \qquad (2.7)$$

Here v_∞ is the velocity of the particles at infinite internuclear separations, and b is the impact parameter. The electron detachment probability is then,

$$P_{DET} = 1 - P_S(b)$$

The total electron detachment cross section is obtained from

$$\sigma_{DET} = 2\pi \int_0^{b_0} [1 - P_S(b)]\, b\, db \qquad (2.8)$$

Where the impact parameter b is the same as given by equation (2.2). In equation (2.7), E is the center of mass collision energy. In order to calculate the total electron detachment cross section, one has to choose some suitable form of the real and the imaginary part of the interaction potentials as mentioned in equation (2.5). A complete test of the theory will be described later in chapter 4.

2.5 ZERO RADIUS POTENTIAL THEORY.

Transitions are possible between the negative ion (A^-+B) and continuum (A + B + e) states, even when this is not in the unbound degenerate region due to the time dependence of the interaction. This is called dynamic coupling, and, since the time dependence of the interaction is derived from the collision velocity, this type of transition increases with the beam energy. It is largest in the region where the negative ion is nearly unbound. The wave function of the electron which is bound to the neutral molecule by a short-range potential acquires dimensions

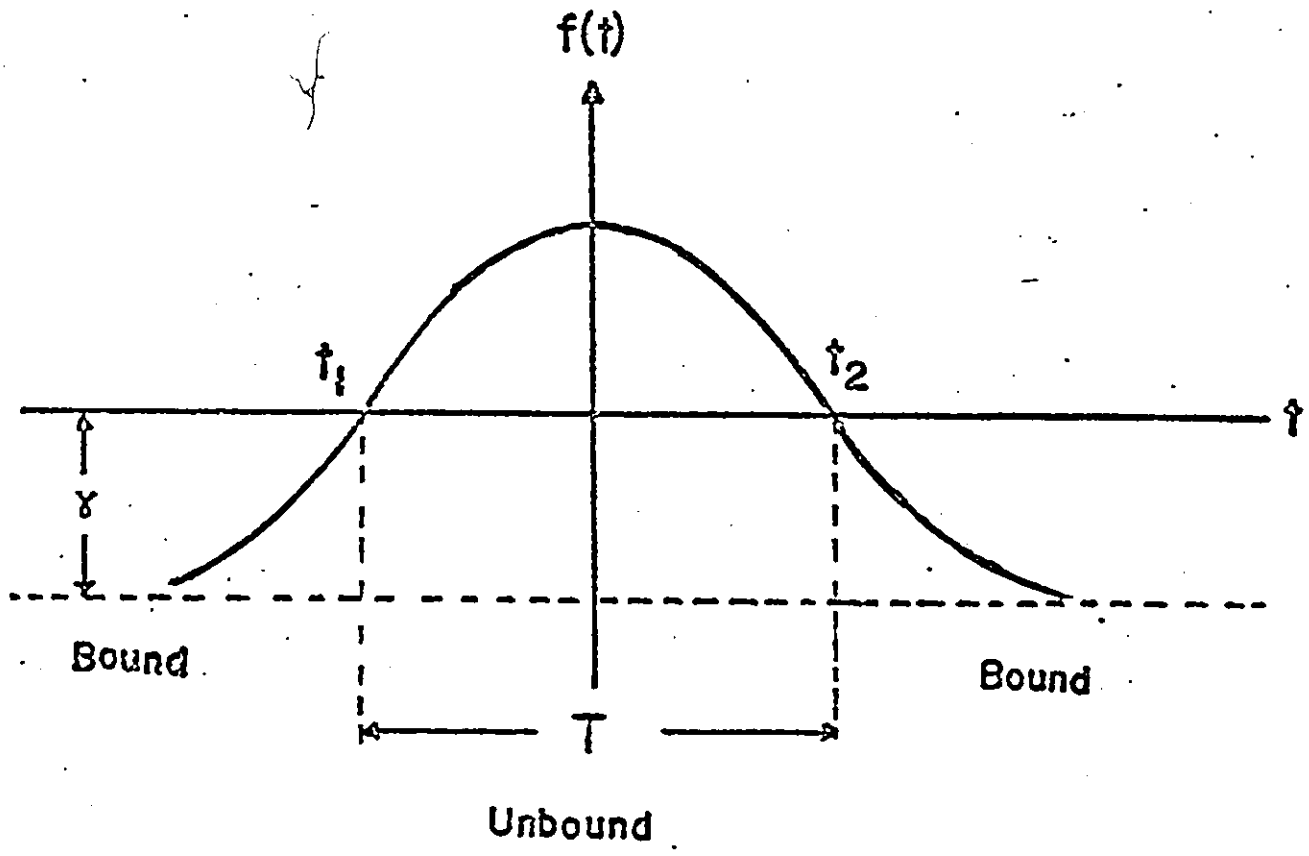

Fig.2.3:- Demkov's zero radius potential approximation showing the variation of f(t) with time.

which more and more exceed the range of the molecular potential as the binding energy decreases. The electron wave function then nearly satisfies the Schrodinger equation for a free particle except over a comparatively localised region. The range of influence of this field may be neglected and effective potential associated with it may be approximately replaced by a zero radius potential well[11], with a time dependent boundary condition to account for variation of the core potential as the internuclear distance changes. The boundary condition is defined by specifying the logrithmic derivative of the wave function at the location of the zero radius potential. The wave function which describes the behaviour of the weakly bound electron, is assumed for simplicity to be spherically symmetric. The non stationary Schrodinger equation for a free particle is

$$i\frac{\partial\psi}{\partial t} = \frac{1}{2}\frac{\partial^2\psi}{\partial r^2} \qquad (2.9)$$

and the boundary condition becomes

$$\frac{1}{\psi}\frac{\partial\psi}{\partial r}\bigg|_{r=0} = f(t) \qquad (2.10)$$

Where all the quantities are assumed to be in atomic units. The situation is illustrated in fig.2.3, for $t \longrightarrow \pm\infty$, and the function $f(t) \longrightarrow \gamma < 0$ where $-\gamma$ is the electron affinity, corresponding to a bound state of the system. For $f(t) > 0$, the potential well is too shallow to bind the electron.

2.6 DEVDARIANI MODEL.

For those collisions where the velocity of relative motion is very slow, so that $R_{min} >> R_o$, the detachment probability is almost zero[5] and the electron remains bound in the negative ion. For the opposite case, $R_{min} << R_o$, Demkov[11] assumed that the detachment probability is unity and f(t) is a linear function of time t, f(t) =-(constant)t. The intermediate case , $R_{min} = R_o$ has been discussed by Devdariani[12]. He assumed f(t) to be a quadratic function of time,

$$f(t) = -\alpha t^2 + \beta \quad , \alpha > 0 , \beta \geq 0 \qquad (2.11)$$

Where $R=R_{min}$ defines the zero of time. In the calculations it turns out that $\lambda = \beta/\alpha^{1/5}$ plays an important role in the detachment probability. The coefficients α and β in equation (2.11) are determined from the time t_1 during the collision when the discrete state merges with the continuous spectrum boundary $f(t_1) = 0$ and from the derivative of f(t) at t_1, so that λ is given by

$$\lambda = \frac{\beta}{\alpha^{1/5}} = \frac{(-t_1)^{6/5}}{(2)^{4/5}} \left[f_t'(t_1) \right]^{4/5} \qquad (2.12)$$

Using the free flight rectilinear approximation and within the semiclassical description of the collision, we obtain

$$\lambda = \frac{\left[b_R'(R_0)\right]^{4/5} R_0^{6/5}}{2^{4/5} v^{2/5}} \left[1 - \frac{b^2}{R_0^2}\right] \qquad (2.13)$$

Where b is the impact parameter. The electron detachment cross section is again given by,

$$\sigma_{DET} = 2\pi \int_0^{\infty} P_{DET}(b)\, b\, db \qquad (2.14)$$

Devdariani found that for $R_0 \approx R_{min}$ and $-1.3 < \lambda < 0.8$, a good approximation was

$$P_{DET} = 0.62 + 0.42\lambda + ORDER(\lambda^2) \qquad (2.15)$$

Substitution of b from equation (2.13) into equation (2.14) gives

$$\sigma_{DET} = \frac{\pi R_0^2}{\lambda_0} \int_{-\infty}^{\lambda_0} P_{DET}(\lambda)\, d\lambda \qquad (2.16)$$

where,

$$\lambda_0 = \frac{\left[b_R'(R_0)\right]^{4/5} R_0^{6/5}}{2^{4/5} \cdot v^{2/5}} = \frac{a}{E^{1/5}} \qquad (2.17)$$

and

$$a = \frac{\left[b_R'(R_0)\right]^{4/5} R_0^{6/5} m^{1/5}}{2} \qquad (2.18)$$

Where m is the mass of energetic negative ion of energy E. In getting equation (2.16) from equation (2.14), the limits also change. The new limits follow directly from equation (2.13), for b=0, $\lambda = \lambda_0$ and for b=∞, $\lambda = -\infty$. Devdariani obtained two different expressions for the electron detachment cross section corresponding to different ranges of λ_0. For $\lambda_0 > 0.9$,

$$\sigma_{DET} = \pi R_0^2 \left[1 + \cdot 29 \frac{E^{1/5}}{a} \right] \qquad (2.19)$$

and with the approximation of equation (2.15),

$$\sigma_{DET} = \pi R_0^2 \left[0.62 + 0.47 \frac{E^{1/5}}{a} + 0.21 \frac{a}{E^{1/5}} \right] \qquad (2.20)$$

In contrast to equation (2.3) which gives a constant value for the cross section in our energy range, the equations (2.19) and (2.20) show a cross section which increases with energy.

2.7 GAUYACQS MODIFICATION.

The use of an analytic function f(t)= -(constant)t by Demkov[11] and $f(t) = -\alpha t^2 + \beta$ by Devdariani[12] was moderately successful in the study of the dynamic electron detachment mechanism. These functions give analytic solutions for the electron detachment probability in terms of α and β parameters. Gauyacq[22] has pointed out that for H^- + He collisions these formulations do not produce satisfactory results. He replaced the

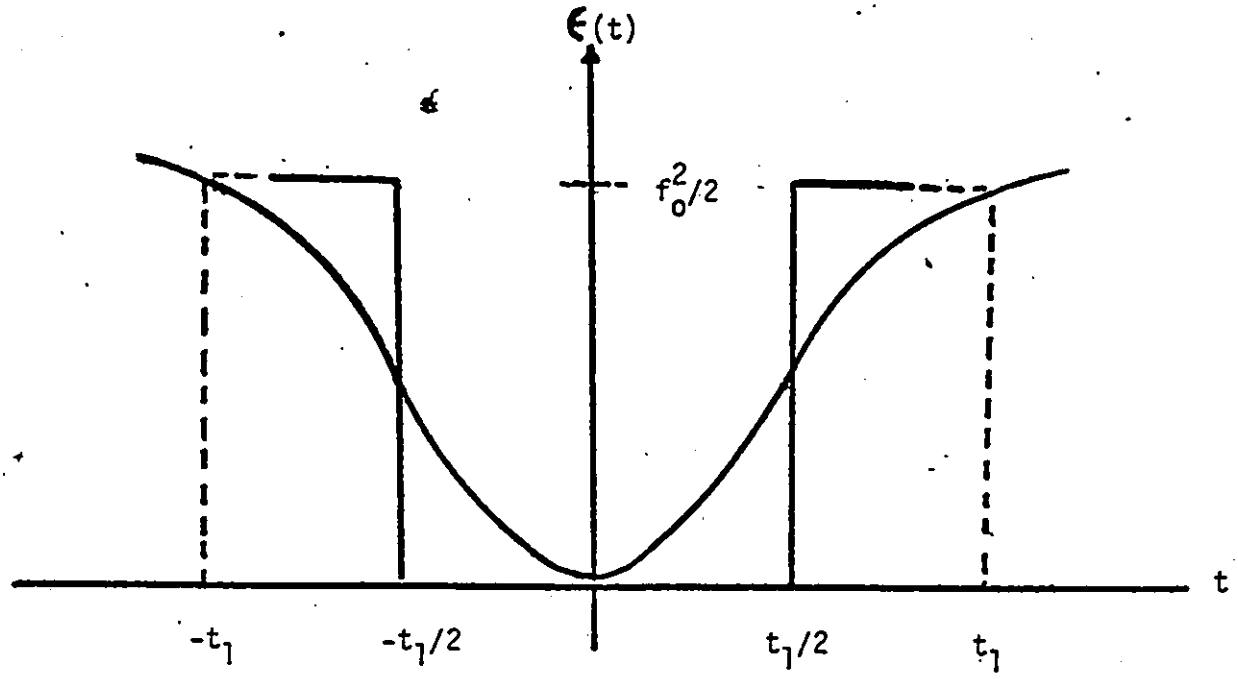

Fig.2.4:- Gauyacq's step function sudden approximation.

smoothly varying function f(t) by a step function which goes discontinuously from the f value at $t = t_1$, to the value at t=0 and he located the step at the mid point between $t=t_1$ and t=0 (fig. 2.4). f(t) was derived from the self consistent field calculations of Olson and Liu[21] which provide the potential energy V(R) and the binding energy ϵ (R) for the electron in the H^-+He, H^-+Ar and Cl^-+Ar systems. Using standard barrier reflection relations, he was able to find the proportion of negative ions which survived the square well, and hence those which did not. The latter were assumed to contribute to the detachment cross section. The characteristic time was defined by equating the time variation of Hamiltonion $\epsilon\left(d\epsilon/dt\right)^{-1}$ with oscillation period of the bound electron, $\frac{1}{\epsilon}$ so that

$$\frac{1}{\epsilon} \cdot \frac{d\epsilon}{dt} = \epsilon \qquad (2.21)$$

Changing the time variable to the internuclear separation R this equation becomes

$$\frac{d\epsilon}{dt} v_\infty \left[1 - \frac{V(R)}{E} - \frac{b_c^2}{R^2}\right]^{1/2} = \epsilon^2 \qquad (2.22)$$

Where v_∞ is the velocity of the particle at infinite internuclear separation. The analytic solution of this equation within the limit of the straight line approximation can be obtained easily and the characteristic time at the distance of closest approach is

$$t_1 = \frac{(R_M - R_0)}{v_\infty}\left[1 - \frac{V(R_M)}{E} - \frac{b_c^2}{R_M^2}\right]^{1/2} \qquad (2.23)$$

Here R_0 is the crossing distance and R_M is the measure of the active region which increases with increasing collision energy. Using the analytic wave functions in the constant potential region on either side of the sudden variation, he obtained the following expression for the survival probability of negative ion,

$$P_s = \frac{16}{\pi^2}\left|\int_0^\infty \frac{e^{-iax^2}}{(1+x^2)^2}\,dx\right|^2 \qquad (2.24)$$

Where $a = 1/2\ f_0^2 t_1$, $f_0 = \sqrt{2\epsilon(R_M)}$. By taking b_{th} as the threshold impact parameter, the total electron detachment cross section is then

$$\sigma_{DET} = \pi b_{TH}^2 (1 - P_s)$$

where $(1 - P_s)$ is the mean detachment probability. The formalism will be discussed in detail later in chapter 4 while applying to the Cl^- + Ar collision case.

2.8 APPROXIMATION FOR WEAKLY BOUND NEGATIVE IONS.

Lopantseva and Firsov[27] have treated the case where the velocity of the ion is much greater than the extra bound electron

velocity in its classical Bohr orbit. Using the idea of Demkov and perturbation methods, they found an expression for the detachment probability of the electron from those negative ions where electron is bound very weakly to the atom. Their formalism is applicable to the alkali metal negative ions colliding with rare gases. They also pointed out that in this case the electron detachment cross section from negative ions equals the cross section for the elastic scattering of slow electrons by a rare gas atom, which is given by

$$\sigma = \frac{4\pi}{\beta^2}$$

here $1/\beta$ is the scattering length of electrons for the rare gas atoms involved. This approach is not suitable for those negative ions in which the extra electron have relatively greater binding energy and the collision velocity is smaller than the extra bound electron velocity in its orbit.

CHAPTER 3

EXPERIMENTAL TECHNIQUE

3.1 EXPERIMENTAL ARRANGEMENTS.

The apparatus used for single and double electron detachment cross section measurements consists of a 150 kV accelerator (Model 150-IH, Texas Nuclear Corporation Austin, Texas), a 90^{o} deflection, 66 cm radius double focusing magnet (Model 90-26, High Voltage Eng. Corporation), and a scattering chamber consisting of a target gas cell and three channeltron electron multipliers as particle detectors. A diagram of the equipment is shown in fig.3.1. The total beam line is 10 m long, provided with four diffusion pumps at different positions. The vacuum attained by these pumps was between 10^{-6} to 10^{-7} Torr along the beam line.

3.2 SCATTERING CHAMBER GEOMETRY.

The scattering chamber was the same as used before for the previous positive ions charge exchange cross section measurements[28] except for some geometrical changes and the replacement of Faraday cup detectors by channeltron detectors. The detector replacement was necessary because the Faraday cup

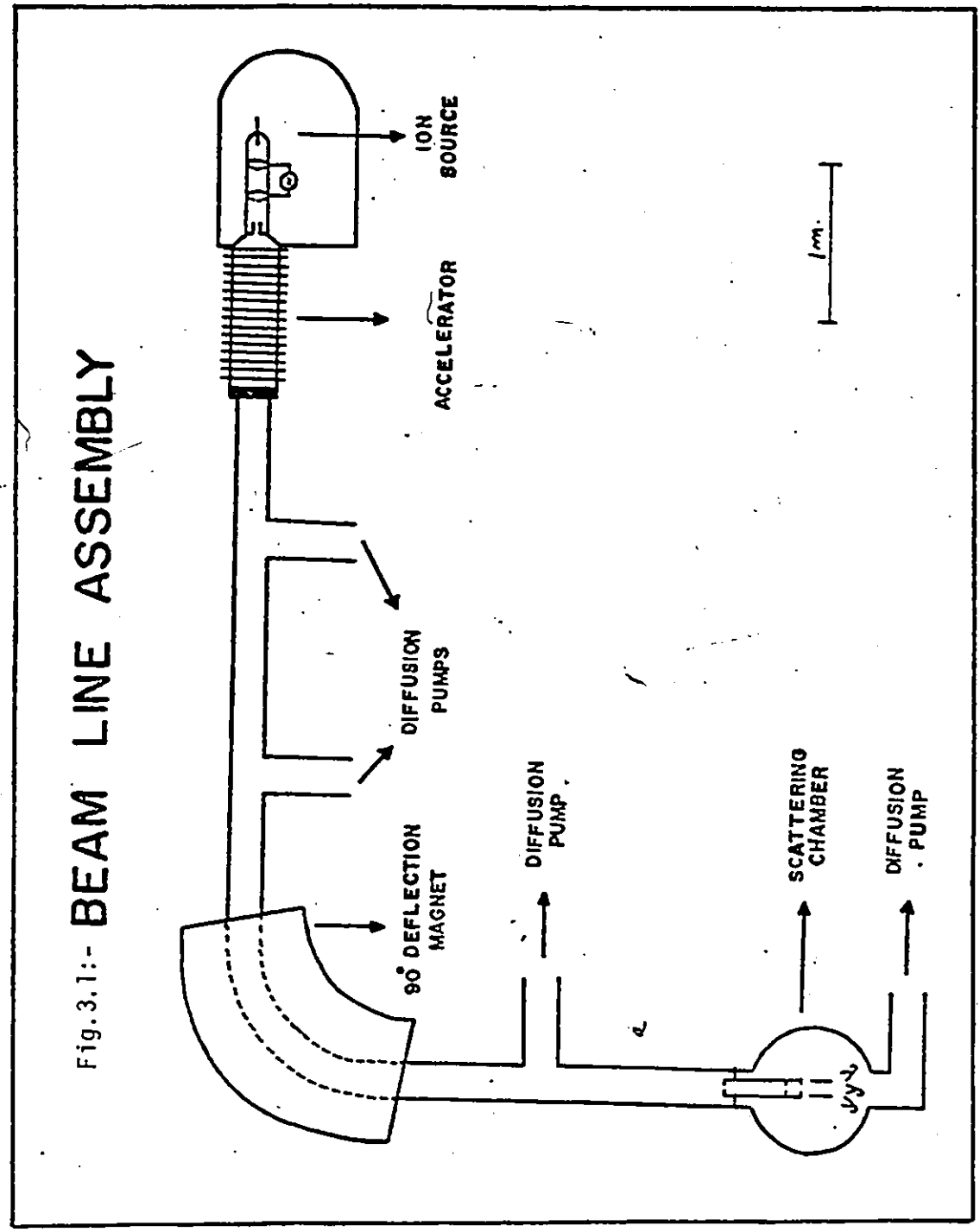

Fig.3.1:- BEAM LINE ASSEMBLY

detector was not sensitive enough to measure the smaller currents from some of negative ion beams. The scattering chamber has a cylindrical geometry with a 36 cm inner diameter and 15 cm inner height. The top and the base of the chamber are symmetrical and each has an internal rotating platform of 35 cm diameter, which could be rotated from outside the chamber. The collimator, electrostatic deflector and channeltrons were mounted on the rotating base platform. The locations of the channeltrons and the other target geometry was calculated carefully. A diagram of the interior of the chamber is shown in fig.3.2. Collimating slits A and B were each 0.8 mm in diameter and were 20 cm apart, thus defining the incident beam direction to a cone of 0.5^{o} full angle. Slit B serves as the entrance to the differentially pumped target gas cell, 3.81 cm in length, with a 1.5 mm diameter slit C as a beam exit port. The dimensions of the target gas cell were a compromise between the requirement that few multiple collisions should occur, that the fast atoms and ions after the collision could escape, and that the pressure range of the target gas was reasonable to give sufficient numbers of detached atoms. Possible end corrections with slits .8 mm and 1.5 mm in diameter were considered small and were neglected. Two tubes were connected through the target cell wall, at right angle to each other, one was connected to the gas supply bottle through a thermal mechanical leak, and the second tube led to the target pressure gauge. Just after the slit C and 2 cm from it an electrostatic

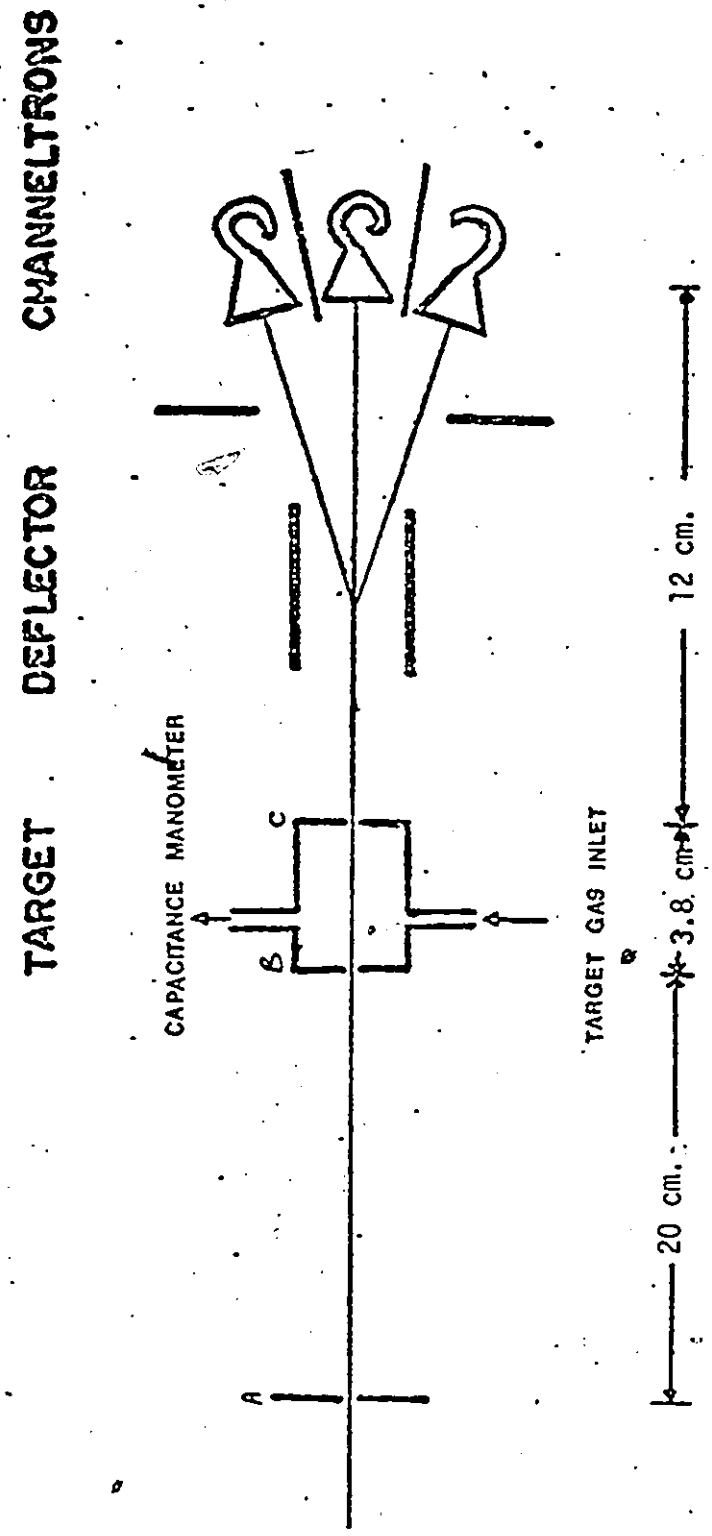

Fig.3.2:- Target system geometry.

deflector was used to separate the various charged components of the scattered beam, as it emerges from the target region through slit C. The distance between the target gas cell and the channeltron detector was 12 cm. The aperture of each channeltron is 1 cm, which makes it possible to collect all those particles which scatter into a cone of 2^{o} half angle. In order to test that most of the scattered particles, after electron detachment collisions were collected by the channeltron detectors, the following test was performed. The straight through channeltron detector was moved one meter away from the target cell and neutral particle distribution was measured in a plane perpendicular to the incoming beam direction at our lowest energy of 10 keV. It was found that more than 90% of the particles were scattered into a cone of 2^{o} half angle and were thus collected by the channeltrons when at their 12 cm position. Three channeltrons used were, a Phillips B419B101 at the undeflected position of the beam line and at one side while a Bendix 4039C was used at the other side position. The central channeltron counted the neutral beam, whereas other two, placed symmetrically on either side counted the negative and the positive ion beams. All the three channeltrons were alligned carefully with the vertical height of the beam line and at the same deflection angle. Each channeltron was separated from the other by an aluminum partition. If the channeltrons were placed so that their cones could 'see each other', then it was found

that coincident pulses were sometimes produced by a single incident ion due to secondary electrons being transferred from one cone to another. Similarly, secondaries from any projecting metal surface which intersected the ions in front of a cone, were counted. The solution was found to be to locate the front of all three channeltrons and the front of the aluminium separator carefully along a common plane. All three were kept in a grounded metalic enclosure with a 2.5 cm diameter window for beam entrance. Since channeltrons are sensitive to light, all transparent viewers on the scattering chamber were replaced by opaque covers.

3.3 INITIAL GROWTH METHOD.

The initial growth technique was used in finding the single and two electron detachment cross sections from negative ions in collision with rare gas atoms. If a beam of negative ions is passed through a thin target, then the emerging charge composition of the beam depends linearly on the atoms per unit area of the target. The measured rate of change of each charge component of the beam with target pressure for a known constant target thickness, gives the cross section of the various processes.

The single and two electron detachment cross sections can be determined experimently by the relation,

$$\sigma_{ij} = \frac{N^j}{N^i} \times \frac{1}{nL} \qquad (3\cdot1)$$

For the single electron detachment cross section, i=-1, j=0, N^0/N^- is the ratio of the neutral particles produced during the collision to the total number of negative ions passing through the target of atomic density n and effective length L, the product nL is known as the target thickness. Similarly for double electron detachment cross section j=+1. This thin target approximation neglects multiple collisions, so is only exactly true for an infinitly thin target. For a practical thin target where a small proportion of ions make double collisions, the theory will be developed later. The condition that a target can be considered as thin is that

$$nL \sum_i \sigma_{ij} \ll 1$$

3.4 EXPERIMENTAL PROCEDURE.

The equipment can be used for both, positive as well as negative ion-atom collision studies. In order to use either of these beams, the polarity of the voltage of the following equipment has to be changed,

1. Accelerator
2. Extractor voltage from the ion source

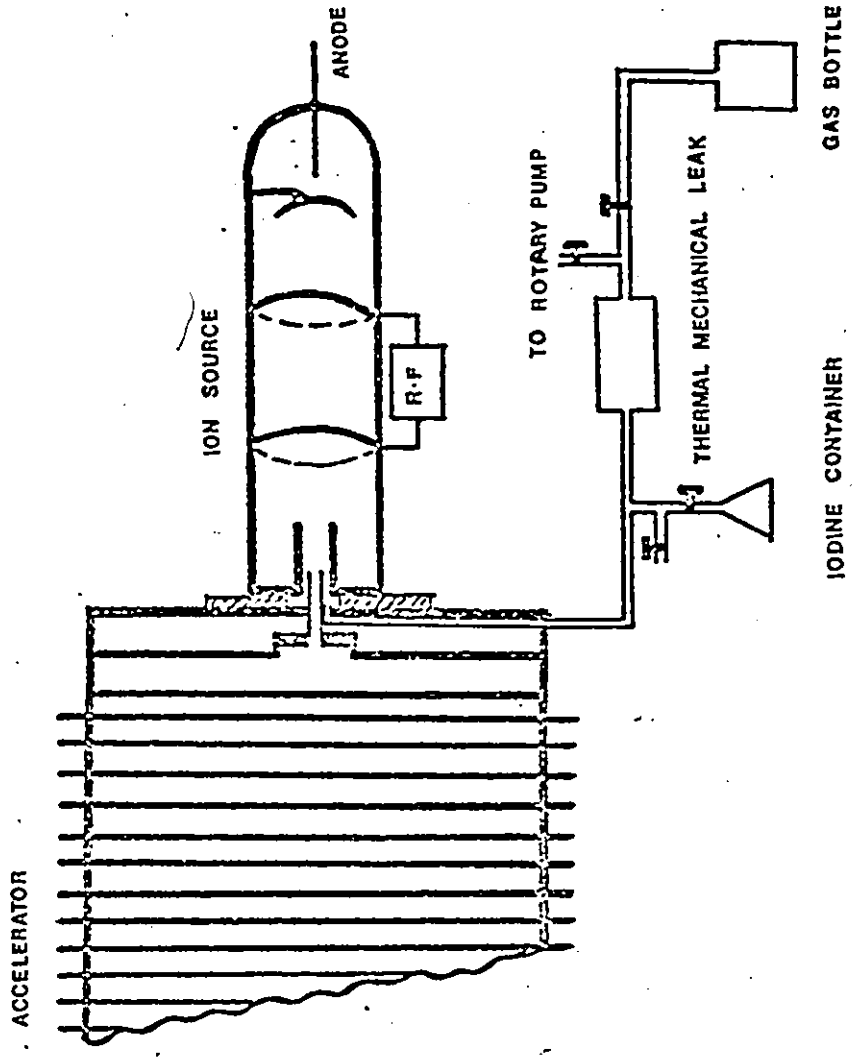

Fig.3.3:- Gas supply to the ion source.

3. 90^{o} deflection magnet

A sufficient beam of negative ions was obtained from a radio frequency type of ion source without changing its polarity and negative ions were presumeably produced from positive ions in the extraction canal region by electron capture collisions. It was found that for the fluorine negative ions beam, the optimum ion source conditions required somewhat higher than normal gas pressures and higher anode voltages and their adjustment was found to be more critical than was the case for other negative ion beams studied. The fig.3.3 shows the gas supply to the ion source. The F^{-} and Cl^{-} ions beams were obtained by using a commercially available Freon 12 gas($C Cl_2 F_2$), whose aerosol cylinder was placed inside a bellows having a sharp needle at the center of its closed bottom end. The other end of the bellows was blanked off with a cover having a control valve leading to the thermal mechanical leak. The previously evacuated bellows was squeezed, thus puncturing the gas cylinder inside the bellows, and the valve to the thermal mechanical leak was opened to fill it to some suitable pressure and then was kept shut. The ion source was then fed with gas through thermal mechanical leak. To obtain the I^{-} beam, iodine crystals were placed in an extra glass tube connected directly to the ion source. This tube was pumped after putting the iodine crystals in. The procedure was to leave the tap to the ion source open overnight. During the experiment this tap was kept shut and the ion source was run

Fig.3.4:- Negative ion mass spectrum.
Energy:- 90 keV.

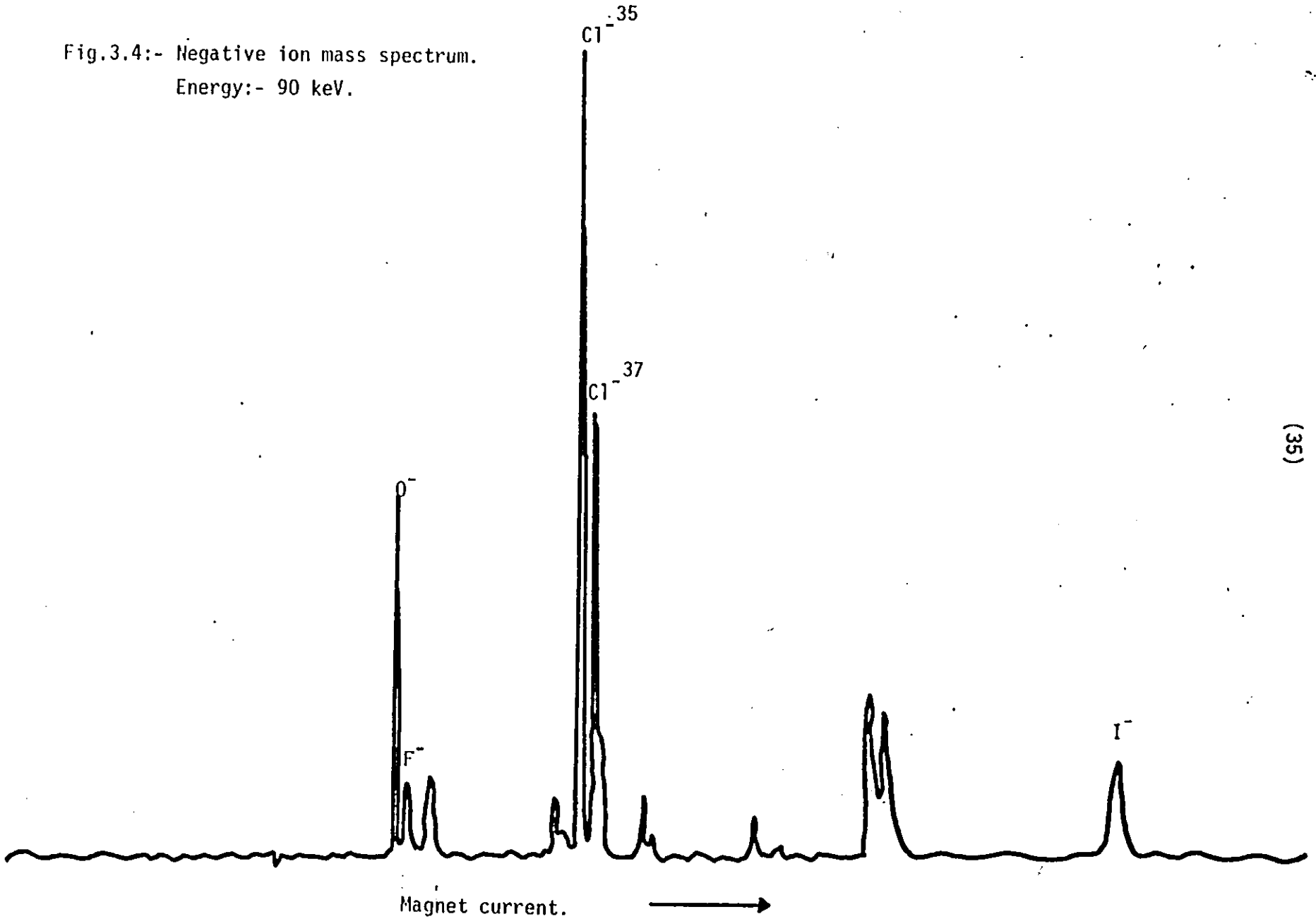

supplied through the thermal mechanical leak. The iodine formed on the surfaces was sufficient to produce the beam during the day. With the tap open during measurements there was less beam, probably because the iodine partial pressure was too high. The mass analysis of the beam was made by 90^{o} deflection magnet. One such mass spectrum plot is shown in fig.3.4. The distance between the magnet exit slit and the target gas cell was chosen in such a way that the center of the target gas cell lies at the image focus point of the magnet.

The negative ion beam selected by the magnet and collimated by slits 'A' and 'B' enter the gas target (fig.3.2) where the target gas pressure was varied in steps. The time interval between the pressure changes was kept sufficiently long to allow the pressure to stabilise. Because all the cross section results are proportional to the target pressure, this had to be known absolutly and with sufficient accuracy. An M.K.S Baratron capacitance manometer with an estimated accuracy of $5X10^{-6}$ Torr was used. This estimated accuracy is suggested by the manufacturer. The absolute calibration of the capacitance manometer was checked by connecting a second identical new manometer through a separate pipe into the target. A difference of about 3 % was found in their absolute calibrations. The pressure inside the target gas cell was always restricted to less than $8X10^{-4}$ Torr. The incident negative ion beam intensity was adjusted so that the neutral atoms and the positive ions rate

were high enough to keep the dark count relatively small and at the same time the negative ion rate was kept below 1 kHz as to avoid pulse pile up problems.

3.5 TARGET THICKNESS CORRECTION.

Corrections for multiple collision in the target can be made, using the series solution method[29], if the proportion of multiple collisions is kept to a few percent. The target thickness in atoms per unit area Π is obtained from the ideal gas equation of state

$$\Pi = \frac{NLP}{RT} \qquad (3.2)$$

Where N is Avogadros number, L is the length of the target gas cell, P is the target gas pressure, R is the gas constant and T is the Kelvin temperture. For numerical calculations

$$\Pi\,(\text{Atoms/cm}^2) = \frac{9.66\times10^{18}\times L\,(\text{Cm})\;P\,(\text{Torr})}{T\,(\text{Kelvin})}$$

The variations in the charge state of an ion beam traversing through a target material of thickness Π is given by[30]

$$\frac{dN^j}{d\Pi} = \sum_{i\neq j}\left[\sigma_{ij}N^i - \sigma_{ji}N^j\right] \qquad (3.3)$$

Where N^j is the fraction of ions in the charge state j and N^i is the fraction of ions in the charge state i of the beam. We can

include the term i=j in the summation of equation (3.3), by writing

$$\frac{dN^j}{d\pi} = \sum_i \sigma_{ij} N^i \qquad (3.4)$$

Where

$$\sigma_{jj} = -\sum_{i \neq j} \sigma_{ji} \qquad (3.5)$$

has been subsituted for the second term of equation (3.3). The integration of equation (3.4) results in exponential functions, but it is possible to obtain a power series solution when π is small. Using the initial boundary condition namely, at X=0, $N^i = N^i$, $N^j = 0$, the solution of equation (3.3) is given by[29]

$$N^j = N_0^i \left[\delta_{ij} + \sigma_{ij}(\pi) + \frac{1}{2}\left(\sum_k \sigma_{ik}\sigma_{kj}\right)(\pi)^2 + \frac{1}{6}\left(\sum_{k,l} \sigma_{ik}\sigma_{kl}\sigma_{lj}\right)(\pi)^3 + \cdots\cdots \right] \qquad (3.6)$$

Neglecting the cross sections for the transfer of three or more electrons and making use of equation (3.6) for the case i=-1 and j=0, we get

$$N^0 = N_0^- \sigma_{-0} \pi \left[1 + \frac{1}{2}\left(\sigma_{00} + \sigma_{--} + \frac{\sigma_{-+}\sigma_{+0}}{\sigma_{-0}}\right)\pi \right] \qquad (3.7)$$

Similarly by taking j=-1, i=-1 in equation (3.6), we get

$$N^- = N_0^- \left[1 + \sigma_{--}(\pi) + \frac{1}{2}\left(\sigma_{--}^2 + \sigma_{-0}\sigma_{0-} + \sigma_{-+}\sigma_{+-}\right)\pi^2 \right] \qquad (3.8)$$

Now neglecting the π^2 term in equation (3.8), dividing equation (3.7) by it and using the binomial expansion we obtain,

$$\frac{N^0}{N^-} = \sigma_{-0}\pi\left[1-\sigma_{--}(\pi)+\frac{1}{2}\left(\sigma_{00}+\sigma_{--}+\frac{\sigma_{-+}\sigma_{+0}}{\sigma_{-0}}\right)\pi\right]$$

Where the expression with π^3 is neglected. Now using equation (3.5) in the last expression for σ_{00} and σ_{--} we get

$$\frac{N^0}{N^-} = \sigma_{-0}\pi\left[1+\frac{1}{2}\left(\sigma_{-0}+\sigma_{-+}-\sigma_{0-}-\sigma_{0+}-\sigma_{02}+\frac{\sigma_{-+}\sigma_{+0}}{\sigma_{-0}}\right)\pi\right]$$

This equation is further simplified as

$$\sigma_{-0} = \frac{N^0}{N^-}\times\frac{1}{\pi}\left[1-\frac{1}{2}\left(\sigma_{-0}+\sigma_{-+}-\sigma_{0-}-\sigma_{0+}-\sigma_{02}+\frac{\sigma_{-+}\sigma_{+0}}{\sigma_{-0}}\right)\pi\right]$$

Which on rearrangment gives the expression for single electron detachment cross section as

$$\sigma_{-0} = \frac{N^0}{(N^-+N^0/2)\pi}\left[1+\frac{1}{2}\left(\sigma_{0-}+\sigma_{0+}+\sigma_{02}-\sigma_{-+}-\frac{\sigma_{-+}\sigma_{+0}}{\sigma_{-0}}\right)\pi\right] \qquad (3.9)$$

Proceeding in a similar manner, by taking i=-1 and j=1 in equation (3.6), we get an expression for two electron detachment cross section as

$$\sigma_{-+} = \frac{N^+}{(N^-+N^+/2)\pi}\left[1+\frac{1}{2}\left(\sigma_{+0}+\sigma_{+-}+\sigma_{+2}-\sigma_{-0}-\frac{\sigma_{0}\sigma_{0+}}{\sigma_{-+}}\right)\right] \qquad (3.10)$$

In equations (3.9) and (3.10) N^0 is the number of neutral particles and N^+ is the number of positive ions produced during the collisions, whereas N^- is the number of negative ions which were left without charge exchange. It should be noted that the correction for multiple collisions in the target is valid to first order in target thickness for a pure N_0^- incident beam and neglecting triple and higher charge states.

3.6 DATA ANALYSIS

The single and double electrons detachment cross sections were first calculated without taking into account the target thickness correction. Complete data on the cross sections needed in the correction term is not available in most of the experiments studied. Therefore the pressure in the target gas cell was restricted so that the thickness was always below 10^{13} atoms/cm^2, when the double collision terms were kept to a few percent and triple collisions were negligible. A computer program was available to calculate the cross sections from the slope of a linear least square fit to the ratios, N^0/N^- for σ_{-0} and N^+/N^- for σ_{-+} as a function of target gas pressure. A small positive intercept in the linear relation was found which is due to residual gas at about $5X10^{-7}$ Torr pressure in the 3 meter length of vacuum between the end of the magnet and the target which created neutrals and positives before the target. It was assumed that both the σ_{-0} and the σ_{-+} cross sections were the same in the residual gas as for the actual target gas so that this background gas increases the effective target thickness. To first order they do not effect the slope of the linear relation and hence the cross section values. It was noticed that there was considerable cancellation within the correction term resulting in a change of measured cross section by less than 5 %, though individual terms produced 10 % changes. As a check, the cross section values were recalculated omitting the highest pressure

reading in each measurement where the correction was largest. The cross sections were found to change typically by 1 % to 2 % with no prefered sign, well within error estimates.

3.7 PULSE COUNTING SYSTEM.

All the three channeltrons were operated with their cones at ground potential and a sufficiently large positive potential on the collector so as to give a reasonable pulse height distribution. It has been found[31] that when channeltrons are operated with a negative potential on the cone so as to have the collector near ground potential, the loss of electrons to the grounded external region reduces the effective aperture of the cone, unless a negatively biased guard ring is used to repel these electrons back into the cone. To investigate any similar loss, the cone of the channeltron was biased by 200 Volts positive and the positive collector voltage was increased by the same amount. No significant increase in the effective area of the particle detection was found, when a small diameter beam was traversed across the diameter of the cone, and the counting rate was constant out to near the geometric edge.

A block diagram of the pulse counting system is shown in fig.3.5. The pulse amplifiers and the discriminators were all set just above the background noise level and the channeltron bias was raised until the pulse height distribution showed a clear maximum well above the noise threshold. When operated

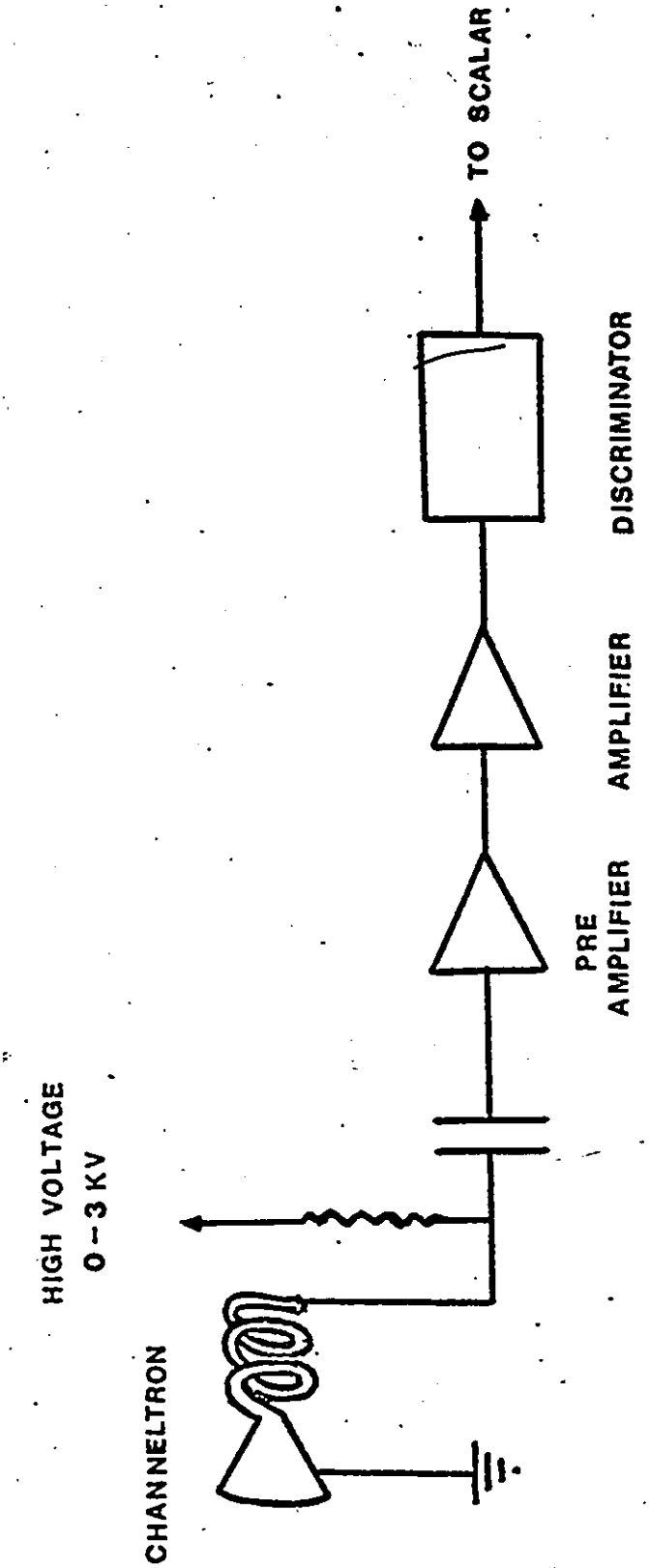

Fig.3.5:- Pulse counting system.

this way the detection efficiencies of the channeltrons were probably near 100 % for the ions and the atoms in this energy range.

3.8 ERROR ESTIMATE.

The total error on these measurements was estimated to come from the following sources,

1. Target gas pressure.
2. Particle collection.

The target pressure was measured on the most sensitive range of the capacitance manometer. It was found that during the three hour run of the experiment there was a drift in the zero reference of the manometer. The error due to this zero drift was minimized in the following way. Before gas was admitted to the target the manometer reading indicating the target residual pressure was noted, then gas was admitted to the target through the thermal mechanical leak in four or five steps up to the highest pressure and measurements were taken at each step. After the highest target gas pressure was reached the process was repeated for descending pressures till the target residual gas pressure was reached and a new reference zero of pressure was recorded. From these two zero reference points an average was calculated and each pressure reading was then corrected with respect to this average zero reference point. The error estimated due to this zero drift was about 2 % for a single experimental

run. An additional 3 % error was estimated from the relative pressure measurements on two similar gauges, one of them was a brand new and recently calibrated by the manufacturer, and the other was in use throughout the last six years.

The channeltrons were set to collect all the scattered particles in 2^{o} half angle cone at the target center. The channeltron effective area was found to be of 9 mm diameter out of its total aperture of 10 mm diameter. This was done by scanning the beam across the channeltron aperture and observing the pulse height distribution. The particle loss, even in the two electron detachment process, at larger angles is not more than 5 %.

The target gases are claimed by the supplier to be pure to 99.99 % and therefore cause no serious error.

All these possible errors make the measured electron detachment cross sections accurate to within 10 %.

CHAPTER 4

RESULTS AND DISCUSSIONS

The σ_0 and the σ_{-+} cross sections are tabulated in tables 4.1 to 4.6 and are shown graphically in figs. 4.1 to 4.6, where they are plotted as a function of incident ion energy. The errors shown are obtained from the addition of 10% instrumental error and those obtained from the least square fit. The error from the length of the target was small and was neglected. However in those cases where the errors resulting from the target thickness correction were relatively large, they were included.

4.1 DATA FOR F^-.

4.1a THE σ_0 CROSS SECTION.

The σ_0 cross section for the F^- + Rg system is shown in fig. 4.1 and tabulated in table 4.1. The previously measured low energy data of Hasted[1] and of Bydin and Dukelskii[5] is also plotted in the same figure for comparision purposes. The data of Hasted (Hollow circles) has a higher values of the cross section at an energy of 4 keV than the present measurements in 25 to 125 keV energy range. The data of Bydin and Dukelskii[5] (Crosses) gives a good extrapolation tp our data. Since Hasted found that his cross section results were dependent on the ion source gas

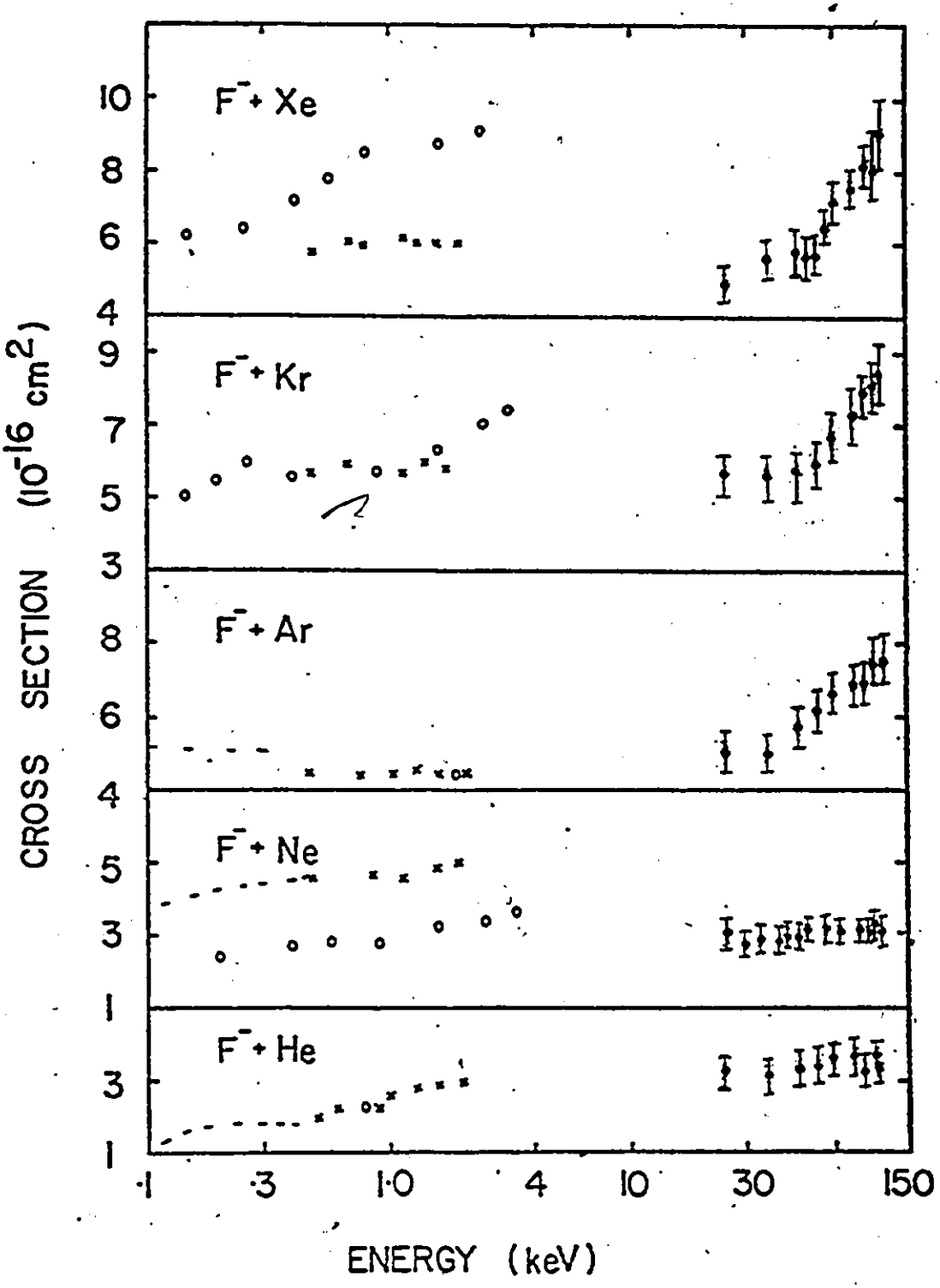

Fig.4.1 :- The single electron detachment cross section σ_0. Crosses are the data of Bydin and Dukelskii[5]. The open circles are the data of Hasted[1]. The dashed lines are the data of Huq et al[32]. The present data are shown with error bars.

which he used to generate the F^- ion beam, it is likely that Bydin and Dukelskii data are more accurate. This is also indicated from a good extrapolation of the lower energy data of Huq et al[32] (dashes) to the data of Bydin and Dukelskii. The σ_{-0} cross section is found to be almost energy independent in He and Ne targets but there is a continuous increase for heavier targets. It should be pointed out that all three previous measurements used the slow electron collection technique, where they effectively measured $\sigma_{-0} + 2\sigma_{-+}$. Our measured σ_{-+} cross section (table 4.2) have its largest magnitude in the He and Ne targets where it is between one third and half of σ_{-0}, thus suggesting that it may be significant throughout the range of energy of Bydin and Dukelskii and up to our lowest energy.

Due to the unavailablity of parameters required for fitting the complex potential model and zero range potential theory, it was not possible to compare the results with theory. De Vreugd et al[33] have observed a stable molecular ion state XeF^- with a life time of 10^{-3} seconds and an electron affinity of .28 eV. This state was observed at an energy of 300 eV and at a scattering angle of 0 to 4 mrad range. In the keV energy range, the collisions are much more violent and this type of long lived association of the colliding partners is very unlikely.

TABLE 4.1:- The cross section for the removal of one electron from a beam of F^- ions by rare-gas atoms (10^{-16} cm^2).

ENERGY (keV)	TARGET				
	He	Ne	Ar	Kr	Xe
25	3.25	3.06	5.00	5.66	4.87
30	-	2.73	-	-	-
35	-	2.89	-	-	-
37.5	3.12	2.84	4.92	5.57	5.58
45	-	2.94	-	-	-
50	3.30	2.94	5.69	5.57	5.81
55	-	3.12	-	-	5.63
60	3.35	3.18	6.17	5.92	5.67
65	-	3.20	-	-	6.43
70	3.61	3.12	6.63	6.67	7.13
75	-	3.04	-	-	-
80	-	3.03	-	-	-
85	3.67	2.89	6.88	7.27	7.52
90	-	3.14	-	-	-
95	3.39	3.13	6.91	7.89	8.18
100	-	3.07	-	-	-
107.5	3.64	3.28	7.48	8.07	8.07
112.5	-	-	-	-	8.60
120	3.22	3.10	7.55	8.38	9.10

4.1b THE σ_{-+} CROSS SECTION.

The σ_{-+} cross sections for the F^- + Rg system are plotted against energy on a linear scale in fig.4.2 and are tabulated in table 4.2. In the same figure are shown the σ_{0+} cross sections measured by Fogel et al[34]. The measured σ_{-+} cross sections have their largest magnitude in lighter targets and are smallest in heavier ones. The general behaviour of the charge exchange cross section is that they are target atomic number dependent in the low energy range. The departure of the σ_{-+} cross section from this general behaviour may be attributed to the projectile and target ionization potentials. The large magnitude of σ_{-+} in He and Ne target may be due to their higher ionization potentials (He=24.58 eV, Ne=21.1 eV) as compared with the ionization potential of fluorine atom (F=17.4 eV). This suggests that after the removal of the first electron from F^-, the second electron removal is more probable from fluorine than from the He or Ne targets. However the situation is not quite the same for the heavy targets, Ar, Kr and Xe which have lower ionization potentials (Ar=15.76 eV, Kr=13.99 eV and Xe=12.13 eV) as compared with the ionization potential of the fluorine atom. In this case target ionization is more favourable than electron loss from the fluorine atom. In negative ions the second electron is more tightly bound than the first electron and its collision with the neutral atom involves crossing of the quasimolecular negative ion state (F^- + Rg) with (F + Rg + e) and (F^+ + Rg + 2e)

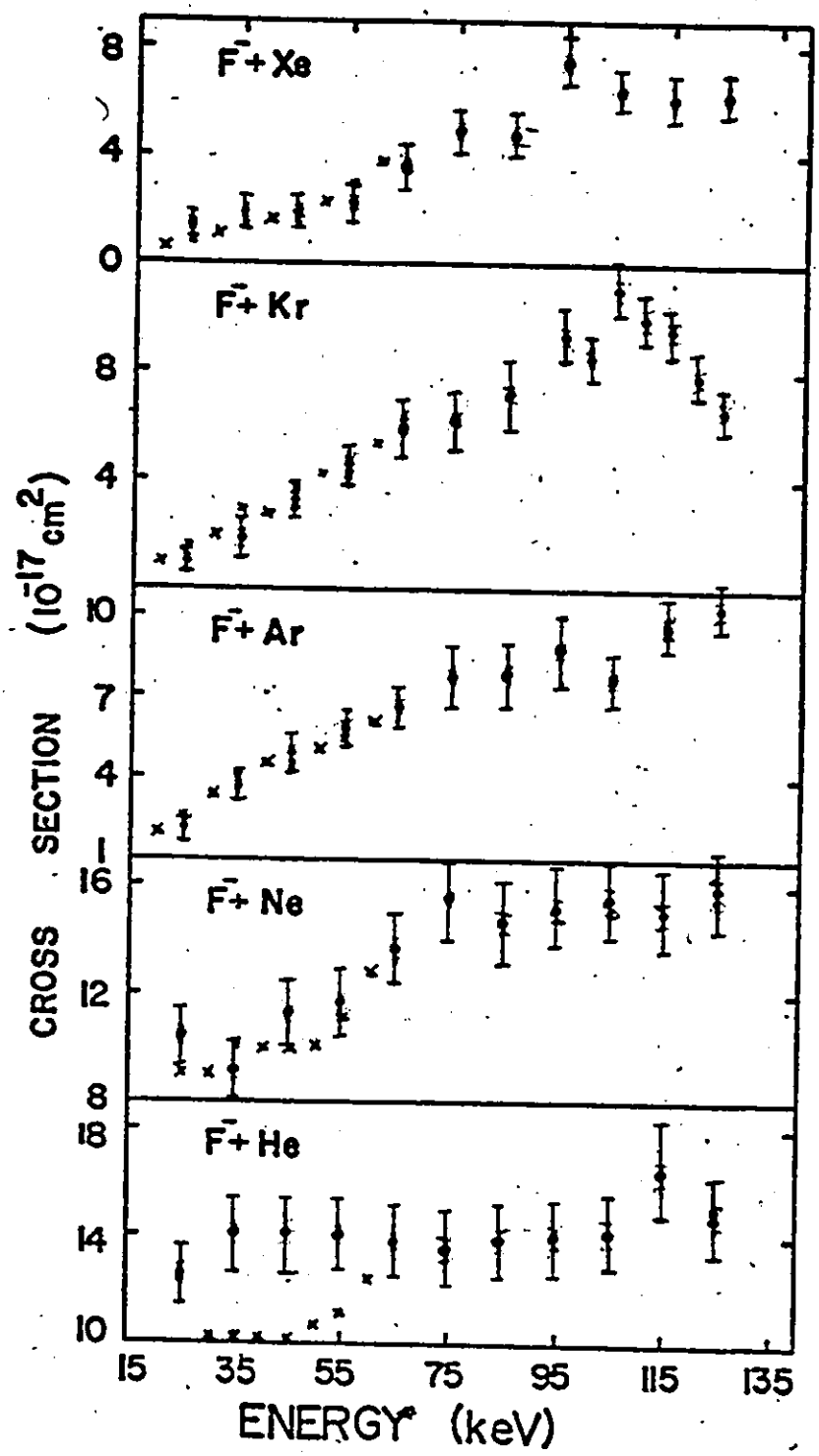

Fig.4.2:- The cross section σ_+ for double electron detachment from F^- in single collision, shown by circles. The crosses are the σ_{0+} cross section measured by Fogel et al[34].

TABLE 4.2:- The cross section for the production of F^+ ions from F^- in single collision with rare-gas atoms (10^{-17} cm^2).

ENERGY (keV)	TARGET				
	He	Ne	Ar	Kr	Xe
25	12.6	10.5	2.22	0.99	1.46
35	14.1	9.19	3.70	1.92	1.91
45	14.1	11.3	4.96	3.31	1.91
55	14.0	11.7	5.88	4.73	2.29
65	13.9	13.7	6.70	6.07	3.73
75	13.6	15.6	7.75	6.35	4.99
85	13.9	14.7	7.85	7.31	4.82
95	14.0	15.2	8.90	9.42	7.59
100	-	-	-	8.58	-
105	14.2	15.6	7.70	11.10	6.52
110	-	-	-	10.00	-
115	16.5	15.1	9.70	9.70	6.15
120	-	-	-	7.94	-
125	14.8	16.0	10.5	6.68	6.26

states. Therefore it is likely that the crossing which leads to the detachment of a second electron occurs at smaller interaction distance than the crossing to the continuum of single free electron states. This means that the second electron detachment occurs, after the negative ion has already lost one electron at larger interaction distance. The very close similarity of σ_{-+} with the σ_{0+} cross section (fig.4.2), both in energy variation and in magnitude for heavier targets confirms this sequental detachment hypothesis. The intresting feature of σ_{-+} and σ_{0+} is that in the He target, σ_{-+} is greater than the σ_{0+} cross section. This may be perhaps due to the formation of some metastable states in the final product of σ_{-+} cross section measurements, which may not be contributing in the σ_{0+} cross section.

4.2 DATA FOR Cl^-.

4.2a THE σ_{-0} CROSS SECTIONS.

The measured σ_{-0} cross sections for the Cl^- + Rg system are tabulated in table 4.3 and are plotted on a logrithmic scale as a function of laboratory energy in fig 4.3. In the same figure are plotted the previously measured low energy data of Hasted[1] and of Bydin and Dukelskii[5]. The energy independent behaviour of the σ_{-0} cross section as observed for F^- ions in He and Ne targets is also present for Cl^- ions incident on these lighter targets. However for heavier rare gas targets there is a

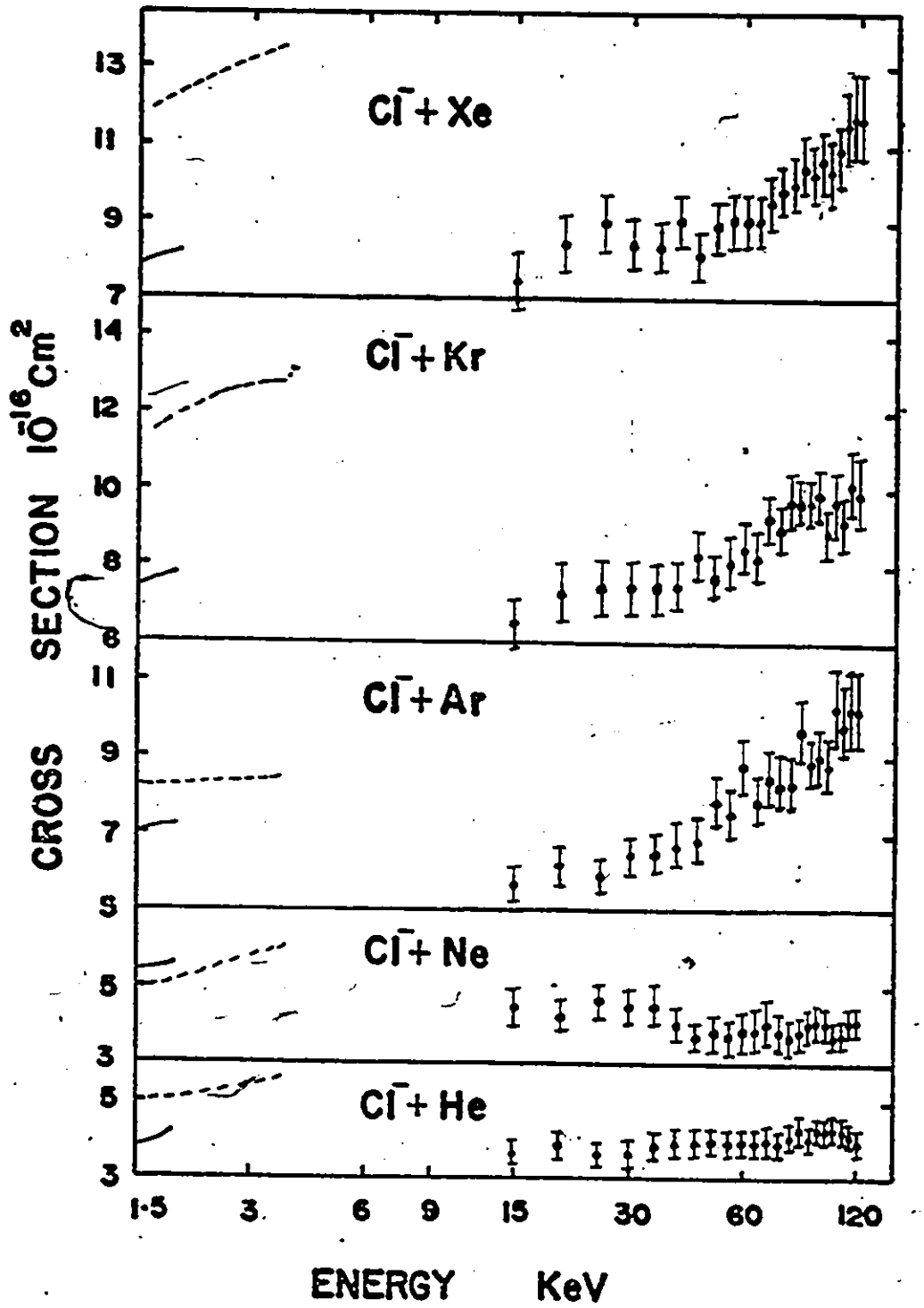

Fig.4.3:- The single electron detachment cross section σ_0. The solid lines are the data of Bydin and Dukelskii[5]. The dashed lines are the data of Hasted[2]. The present data is the solid circles.

TABLE 4.3:- The cross section for the removal of one electron from a beam of Cl^- ions by rare-gas atoms (10^{-16} cm^2).

ENERGY (keV)	TARGET				
	He	Ne	Ar	Kr	Xe
15	3.66	4.53	5.63	6.59	7.57
20	3.83	4.21	6.19	7.38	8.45
25	3.61	4.62	5.94	7.49	9.09
30	3.65	4.49	6.44	7.42	8.50
35	3.82	4.51	6.49	7.60	8.38
40	3.92	4.07	6.68	7.49	9.08
45	3.94	3.71	6.85	8.32	8.11
50	4.04	3.85	7.89	7.67	9.00
55	3.94	3.73	7.56	8.16	9.19
60	4.01	3.91	8.83	8.48	9.16
65	3.94	3.90	7.82	8.24	9.18
70	4.08	4.13	8.51	9.24	9.60
75	3.92	3.86	9.34	8.99	9.84
80	4.16	3.75	8.30	9.78	10.00
85	4.39	3.86	9.79	9.41	10.60
90	4.06	4.04	8.84	9.49	10.30
95	4.33	4.15	9.06	9.91	10.70
100	4.28	4.11	8.80	8.83	10.40
105	4.32	3.75	10.40	9.78	11.00
110	4.31	3.80	9.83	9.17	11.60
115	4.19	4.10	10.30	10.10	11.70
120	4.05	4.16	10.30	9.98	11.70

continuous increase in the cross section with energy. The data of Hasted[1] in the 1.5 to 4 keV energy range has a larger value of the cross section section than the present measurements, but the data of Bydin and Dukelskii[5] up to 2 keV energy provides a good extrapolation to our low energy data, although in some cases its magnitude is slightly higher than the present measurements. As mentioned before, both previous low energy measurements are based on the collection of slow electrons produced during the collision; effectively measuring $\sigma_0 + 2\sigma_+$. However at low energies it may not be contributing sufficiently. Furthermore the data of Hasted is not reliable because of contamination of his Cl^- beam with other gases. It is also evident from tables 4.1 and 4.3 that the σ_0 cross section for Cl^- is bigger than for F^- correspondingly in all rare gases, thus indicating some kind of dependence of cross section on projectiles atomic number.

4.2b PREDICTIONS OF COMPLEX POTENTIAL MODEL.

A comparision of the data with a local complex potential model is shown in fig. 4.3a. The parameters of the complex potential theory were taken from the work of Champion and Doverspike[9]. The real part of the potential used by them was a screened coulomb type of potential,

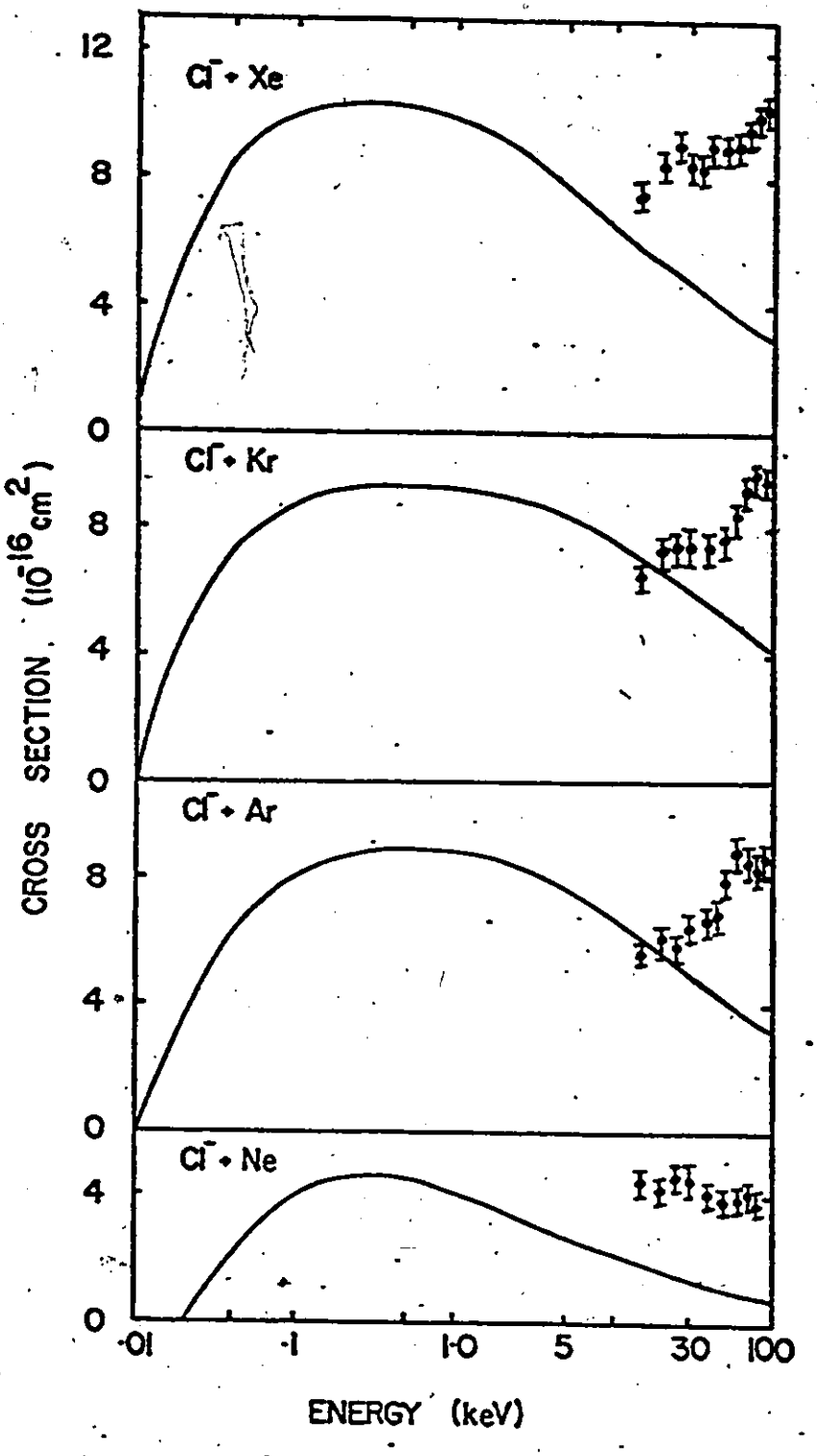

Fig.4.3a:- Comparision between the complex potential model (full curve) and the present measurements (solid circles).

$$V(R) = \frac{A}{R} e^{-BR}$$

Where A and B are constants and R is the internuclear separation. They used the following functional form for the imaginary part of the interaction potential,

$$\Gamma(R) = \begin{cases} 0 & R \geq R_0 \\ F(R_0 - R)^{3/2} & R_1 \leq R \leq R_0 \\ F(R_0 - R_1)^{3/2} & R < R_1 \end{cases}$$

The other parameters used in conjuction with these relations and with the formulation already discussed in section 2.4, are tabulated in table 4.3a The survival probability of Cl^- ions in their collisions with rare gases was calculated by making use of these parameters in equation (2.6). The electron detachment cross section was obtained from equation (2.8). It was found that the detachment cross section calculated from this model increases with energy from threshold to a few hundred eV after which it decreases throughout the range of energy of the present measurements to a value which is much less than the measured experimental cross sections.

TABLE 4.3a The complex potential parameters for Cl^- + Rg.

Target	A	B	R_x	F	R_1
Ne	826	1.39	2.61	4.8	2.40
Ar	2530	1.37	3.39	5.4	3.07
Kr	3062	1.39	3.46	4.6	3.00
Xe	4530	1.36	3.73	2.0	3.25

4.2c PREDICTIONS OF THE ZRP THEORY.

In contrast to the complex potential model, the Zero Range Potential theory includes quantum mechanical tunneling and provides a better fit with the present measurements for the Cl^- + Ar system. Devdarianis formulation[12] of the Zero Radius Potential theory was used with Gauyacqs modification[22,23] to derive the parameters of the theory. The formalism was outlined in chapter 2. The self consistent field energies, calculated as a function of internuclear separation, by Olson and Liu[21] were fitted to exponential functions for the Cl^- + Ar system. The differences when displaced by the electron affinity give the binding energy $\epsilon(r)$ of the electron to the molecule and predict a crossing radius R_o = 3.4 au to an unbound state and a second crossing back to a bound state at R = 2.7 au. A Morse type function was used for fitting purposes to provide an analytic

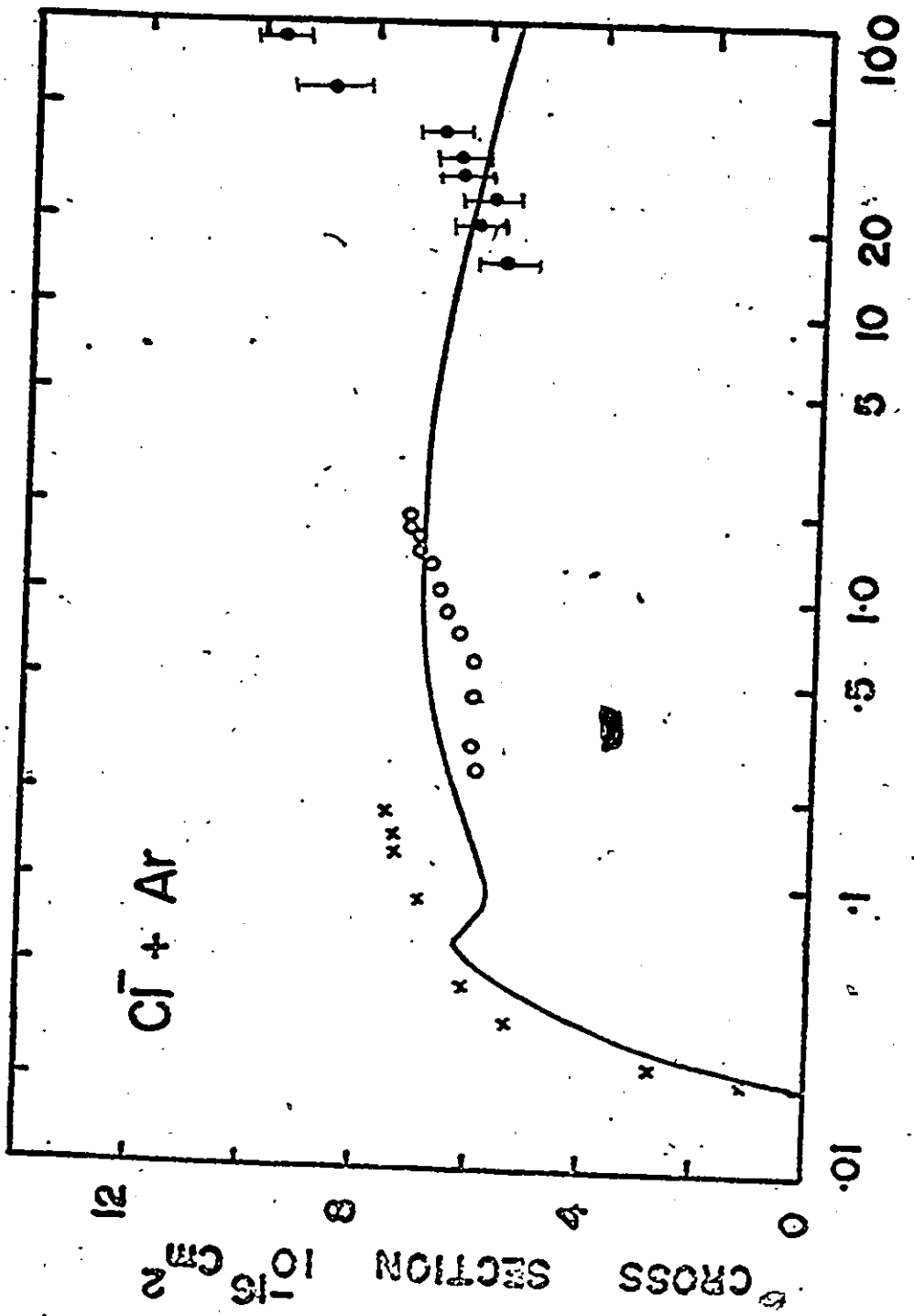

Fig.4.3b:- Comparision between the zero range sudden approximation model of Gauyacq using the molecular energies of Olson and Liu, and the experimental data of Smith et al[10], shown by crosses, the data of Bydin and Dukelskii[5] shown by circles and the present measurements shown by dots.

description of $\epsilon(r)$. For each collision energy the value of R_M and $\epsilon(R_M)$ were extracted from this fitting procedure and the characteristic time t_1 at the distance of closest approach was calculated from equation (2.23). The survival probability of the negative ion was calculated from equation (2.24). The threshold impact parameter b_{th} is determined such that the corresponding turning point R_o verifies $f(R_o) = f_o/3.35$, where $f_o = \sqrt{2\epsilon(R_M)}$. Finally the electron detachment cross section was calculated from equation (2.25).

The cross sections obtained from the theory are plotted in fig.4.3b , where they are compared with the experimental data for the Cl^- + Ar system. There is a dip in theoretical cross section at about 60 keV, this is because at about this energy the distance of closest approach for small impact parameters has penetrated through the unbound region of the molecular ion far enough to reach the bound region at smaller radii. Calculations were made to test the effect of inside region by replacing the Morse function with a Fermi Dirac function fit to the Olson and Liu $\epsilon(r)$ values. The Fermi Dirac function does not become positive at small r values like the Morse function but gives an excellent fit beyond the crossing radius. The cross sections with this function were unchanged at small energies but the dip was absent and the values continued to rise to a higher plateau than when the Morse function was used. The correct energy dependence is probably somewhere between the predictions of the two

functions with a finite but small probability of survival of the negative molecular ion into the inside stable region for small impact parameters. The overal magnitude of the experimental cross sections is fitted quite well by this theory which does not contain any free parameters, in spite of the use of the zero range approximation in a form which is only valid for s-state electron wave functions. This model like the complex potential model does not include the excitation effects occuring along with the detachment process. The rise in the experimental cross section above about 50 keV is probably due to the increased production of excited states of the negative ions and the neutrals. Such states have been identified in the energy loss spectra of Fayeton et al[8] and in the electron spectra of de Vreugd et al[35], who estimated that about 1/40 of the cross section goes by way of the low lying negative metastables at 2 keV beam energy. With increasing energy a higher production of metastable states is expected.

4.2d THE σ_{-+}^{-} CROSS SECTION.

The cross sections for the production of Cl^+ from a Cl^- beam in collisions with rare gases are tabulated in table 4.4 and shown in fig.4.4, where they are plotted against the energy of the incoming Cl^- beam. The σ_{-+}^{-} cross section increases with energy in the lower energy region and then starts showing energy

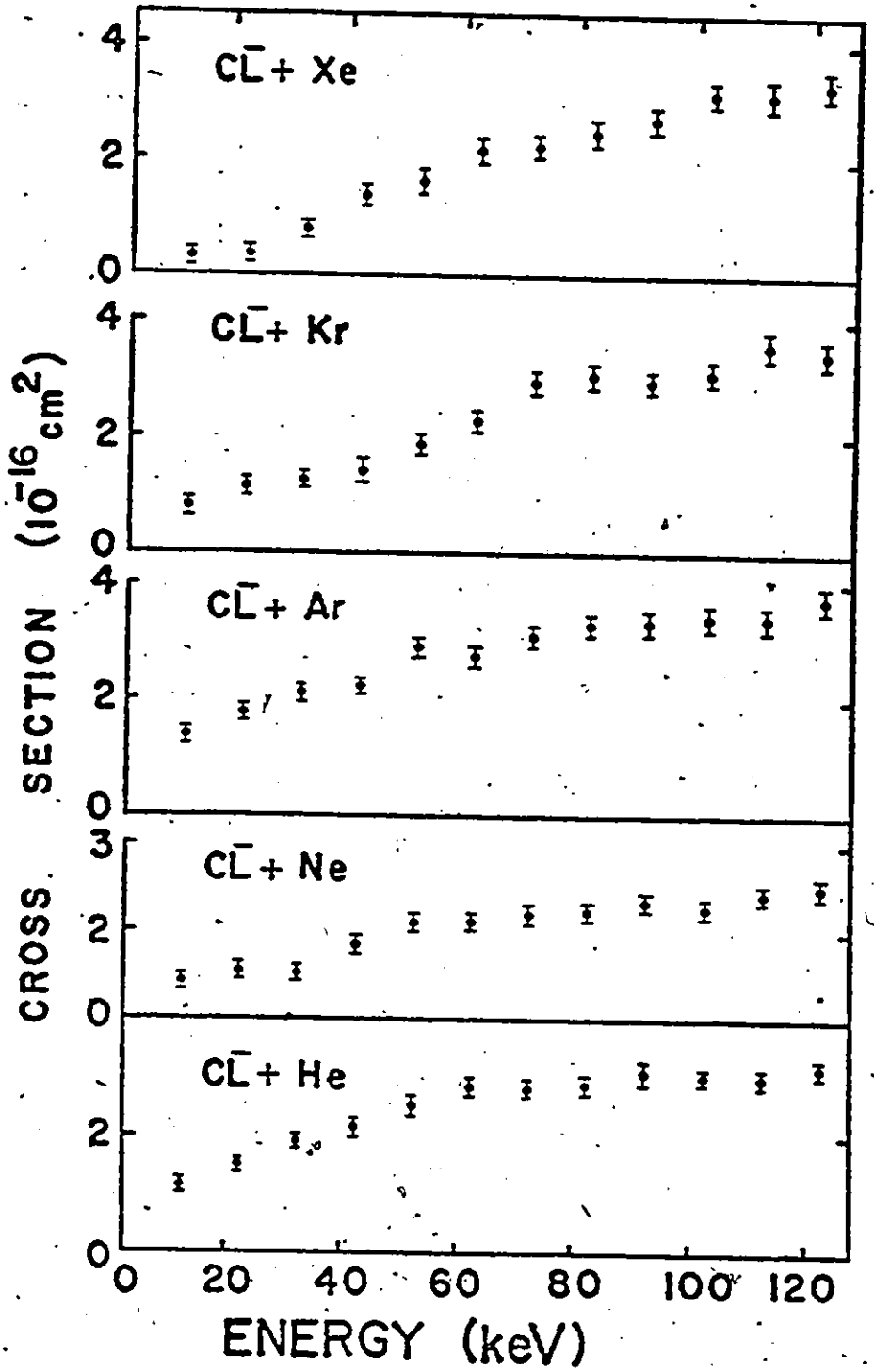

Fig.4.4:- The cross section σ_{-+} for double electron detachment from Cl^- in a single collision with a rare gas atom.

TABLE 4.4:- The cross section for the production of Cl^+ ions from Cl^- in single collision with rare-gas atoms (10^{-16} cm^2).

ENERGY (keV)	TARGET				
	He	Ne	Ar	Kr	Xe
12.5	1.15	0.65	1.38	0.80	0.33
22.5	1.52	0.79	1.78	1.15	0.36
32.5	1.90	0.76	2.14	1.26	0.80
42.5	2.17	1.28	2.22	1.42	1.39
52.5	2.53	1.66	2.92	1.90	1.65
62.5	2.84	1.67	2.76	2.29	2.16
72.5	2.80	1.81	3.11	2.95	2.25
82.5	2.88	1.84	3.29	3.08	2.49
92.5	3.08	2.02	3.34	2.97	2.72
102.5	3.02	1.92	3.41	3.11	3.16
112.5	3.00	2.12	3.44	3.58	3.13
122.5	3.22	2.28	3.75	3.45	3.30

independent behaviour in the higher energy region for all the targets. The σ_{-+} cross sections are found to have their largest magnitude in Ar target but smallest in Ne target. Above 90 keV energy the magnitude of the cross section is almost the same for all the targets but Ne. The inverse atomic number dependence of cross section as observed in the F^- case, is not strong in the Cl^- + Rg system. The ionization potential of Cl atom is 12.97 eV which is less than the ionization potentials of He, Ne, Ar and Kr but greater than for Xe. This indicates that preferential target ionization may occur in the Xe target only. It may also be effective to some extent in the Kr target where the ionization potential differs only by about 1 eV and perhaps it could be a reason that the cross section in Kr and Xe targets have a smaller magnitude than for the Ar target. However in the He target the cross section is smaller than that in Ar throughout the energy range, but not smaller than in the Kr and Xe targets . Above 45 keV energy the cross section in Ne target is the smallest. This suggests that beside preferential target ionization there are other factors as well which make the σ_{-+} cross section behave in an anomalous way. For those beam target combinations where both the σ_{-0} and the σ_{-+} have been measured[15], it has been found that both cross sections have very simillar dependence on collision energy, on the target mass and on the absolute magnitude of the cross sections. While simple detachment seems usually to be the dominant process in most σ_{-0} detachment collisions, it has been

suggested by Fayeton et al[8] that Cl^- + Ar is unusual in that single detachment occurs mostly through the formation of metastable Cl^* ions , which auto detach on their way out, rather than by simple detachment from the ground state. If auto-detachment from excited metastables dominates single detacbment, then it is possible that the first electron from double detachment is also mainly produced in this way. The neutral molecular state left behind would then differ from that formed in neutral neutral collisions and there would be no reason for the σ_{-0} and the σ_{-+} cross sections to be simillar.

4.3 DATA FOR I^-.

4.3a. THE σ_{-0} CROSS SECTION.

The σ_{-0} cross section for the production of neutral iodine atoms, I^0 from negative iodine ions I^- in rare gas collisions is shown in fig 4.5 and are tabulated in table 4.5. Also shown in fig.4.5 are the results of early low energy measurements of Bydin and Dukelskii[5] and of Haywood et al[36]. Lichtenberg et al[24] have measured the σ_{tot} and the σ_{-+} cross section in 20 keV to 220 keV energy range in He and Ar targets. We have plotted in fig.4.5, their σ_{tot} cross section after subtracting their values of the σ_{-+} cross section. These corrected values of their σ_{-0} cross section are in agreement with the present measurements within their estimated error of 20 % in

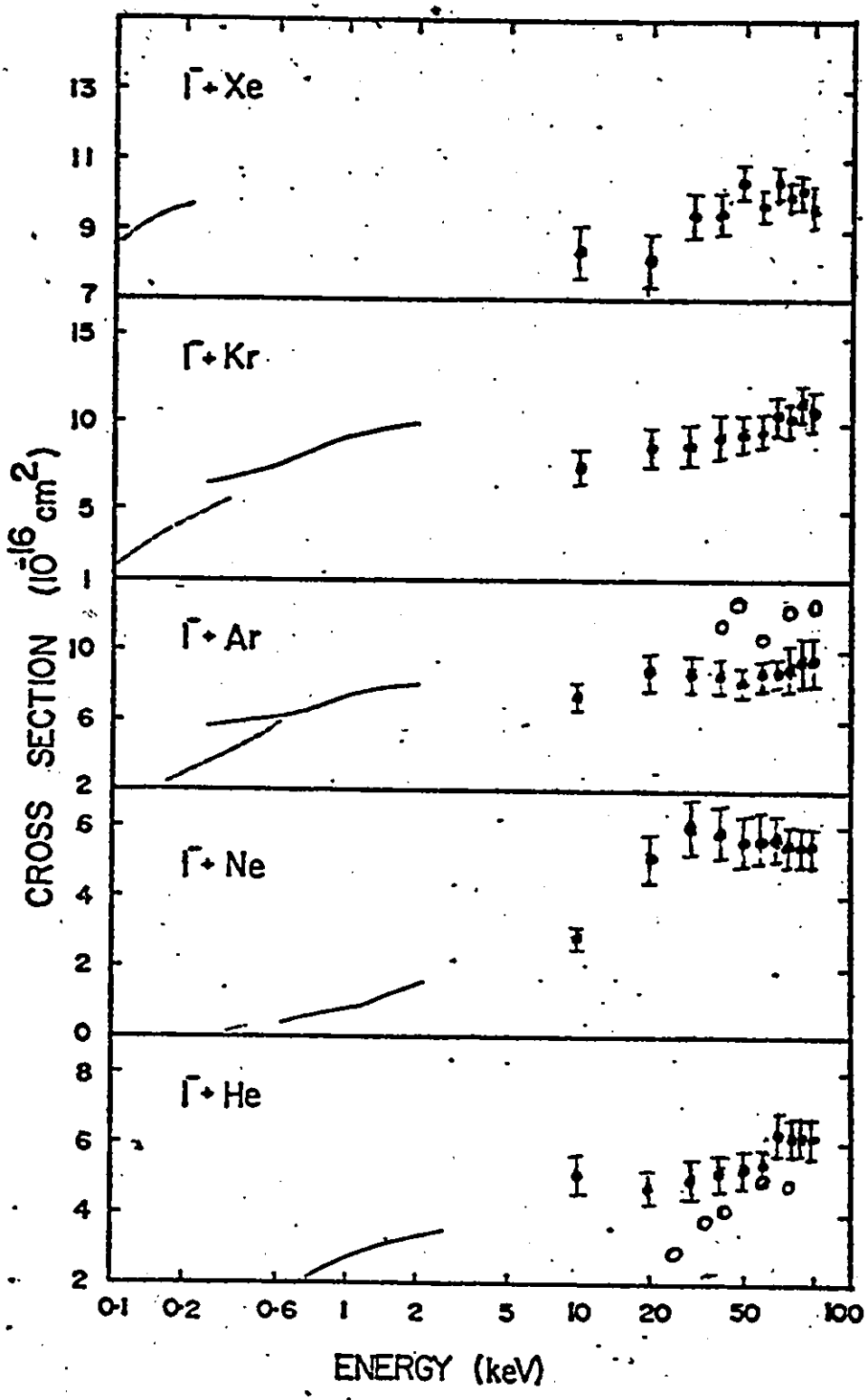

Fig.4.5:- The single electron detachment cross section σ_0. Open circles are the data of Lichtenberg et al[24]. The continuous lines are data of Bydin and Dukelskii[5]. The dashed lines are data of Haywood et al[36]. The present data is shown with error bars.

TABLE 4.5:- The cross section for the removal of one electron from a beam of I^- ions by rare-gas atoms (10^{-16} cm^2).

ENERGY (keV)	TARGET				
	He	Ne	Ar	Kr	Xe
10	5.18	2.83	7.45	7.65	8.45
20	4.82	5.17	8.90	8.90	8.20
30	4.99	6.10	8.83	8.90	9.20
40	5.23	5.89	8.61	9.29	9.53
50	5.32	5.57	8.27	9.51	10.40
60	5.45	5.62	8.85	9.78	9.83
70	6.32	5.78	8.87	10.70	10.40
80	6.20	5.55	9.10	10.40	9.98
90	6.20	5.44	9.58	11.30	10.10
100	6.18	5.45	9.69	11.00	9.66

their data. The increase of the σ_0 cross section with energy is slow as compared with other ion atom combinations. Generally the magnitude of the σ_0 cross section for I^- is bigger in all the rare gases as compared with the corresponding σ_0 cross section for F^- and Cl^- in the same target, the only exception is the xenon target in which both I^- and Cl^- have the same magnitude of the σ_0 cross section. The σ_0 cross section also increases with the target atomic number except for the Ne target throughout our energy range and for the Xe target from 70 keV to 100 keV energy. The unusual behavior of I^- in Ne was first observed by Bydin and Dukelskii[5] in their low energy measurements of σ_0 cross section and later by Haywood et al[36] in their near threshold to a few hundreds eV energy range measurements. Bydin and Ioffe[37] measured the energy spectrum of ejected electrons for the I^- + Rg system and observed that the energy spectrum differs for I^- + Ne from other I^- + Rg systems investigated. They noticed that while other systems have an extra peak at 6-7 eV above the first peak which occurs at 2-3 eV energy, the I^- + Ne system shows only a single peak representing a group of 2-3 eV electrons. They postulated the existance of an autodetaching state of I^- which was later observed by Cunningham and Edwards[38].

The data of Haywood et al[36] in the Xe target increases with energy from threshold to about 190 eV energy after which it is energy independent and is in agreement with the data of Bydin and Dukelskii[5]. The extrapolation of our data with these low

energy measurements is good for Ne, Ar and Kr targets because their cross section is increasing continuously in their energy range and perhaps between their highest energy and our lowest energies as well. However for the Xe target their values are higher than the present measurements and extrapolation is not good unless one assumes that the cross section decreases slowly between their highest and our lowest energy range. No attempt was made to obtain a theoretical fit, because the parameters for neither the complex potential model nor the ZRP theory are available.

4.3b THE σ_{-+} CROSS SECTION.

The σ_{-+} cross section for the I^- + Rg system is shown in table 4.6 and are plotted on a linear scale in fig 4.6. In the same fig. the data of Lichtenberg et al and of Dukelskii and Fedorenko[14] is also shown. The agreement is good except for the He target where present measurements have a larger magnitude. The unusual behaviour of the σ_{-+} cross section as found in F^- + Rg and the Cl^- + Rg collision systems that it has larger magnitude in lighter targets than heavier ones, is not present in the I^- + Rg collision system but instead roughly target atomic number dependence is observed. However in the Ne target the cross section is of smallest magnitude and this behaviour like the σ_{-0} cross section in Ne target, perhaps could be explain if

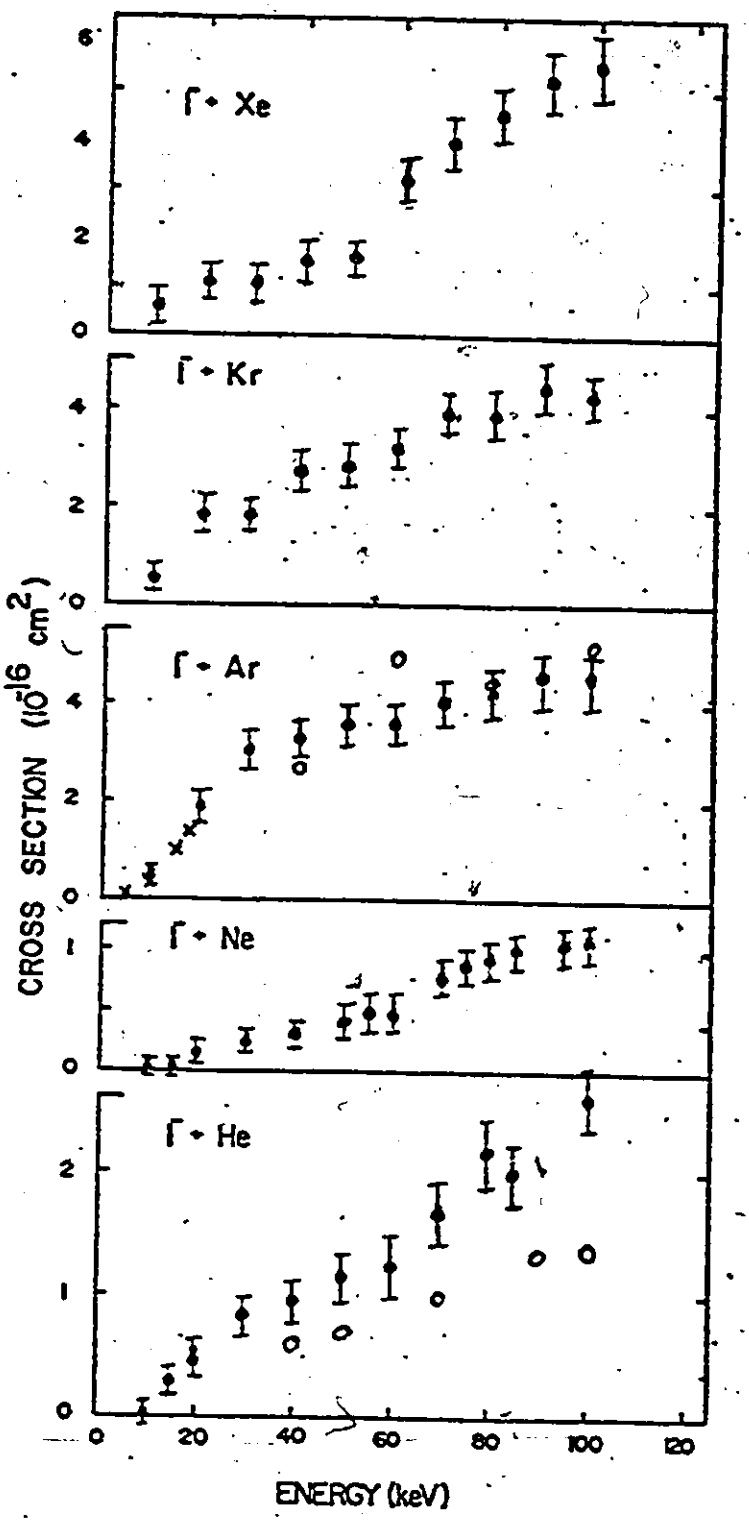

Fig.4.6:- The cross section for the detachment of two electrons in a single atomic collision. The crosses are the data of Dukelskii and Fedorenko.[14] The open circles are the data of Lichtenberg et al [24].

TABLE 4.6:- The cross section for production of I^+ from I^- in single collision with rare-gas targets (10^{-16} cm^2).

ENERGY (keV)	TARGET				
	He	Ne	Ar	Kr	Xe
10	0.09	0.03	0.50	0.46	0.64
15	0.30	0.03	-	-	-
20	0.46	0.14	1.93	1.82	1.24
30	0.83	0.25	3.06	1.83	1.12
40	0.95	0.31	3.28	2.75	1.57
50	1.15	0.40	3.58	2.82	1.60
60	1.23	0.45	3.57	3.23	3.21
70	1.60	0.77	4.07	3.99	3.98
75	-	0.89	-	-	-
80	2.17	0.94	4.25	3.94	4.53
85	2.00	1.01	-	-	-
90	-	-	4.58	4.48	5.25
95	-	1.06	-	-	-
100	2.62	1.08	4.56	4.32	5.55

measurements were made on the spectra of ejected electrons in this energy range. The ionization potential of iodine is smaller than the ionization potential of all the rare gases and therefore the preferential target ionization which caused a reduction in the σ_{-+} cross section for the F^- + Rg and the Cl^- + Rg collision systems, is less probable in the I^- + Rg case. It is observed that the F^- + Rg and the I^- + Rg are the two extreme cases, of the effect of preferential target ionization reducing the magnitude of the σ_{-+} cross section. It is most effective in F^- and least effective in I^-. The Cl^- + Rg and the Br^- + Rg[39] systems show an intermediate behaviour between these two extreme cases.

CHAPTER 5

CONCLUSIONS.

This thesis presents the study of one and two electron detachment cross sections from F^-, Cl^- and I^- ions with rare gases in the multi keV energy range. An improved experimental technique was followed which permitted measurements of the neutral and charged particles directly instead of measuring the slow electrons detached from negative ions during the collision. The use of three channeltrons made it possible to measure both the σ_{-0} and the σ_{-+} cross sections simultaneously and accurately.

The single electron detachment cross section is found to be almost energy independent for F^- and Cl^- in He and Ne targets, whereas for other targets it increases with energy. For the I^- + Rg system the σ_{-0} cross section increases with energy in all targets. It has been observed[39] that for the Br^- + Rg system, the σ_{-0} cross section increases with energy in all targets except Ne where it is almost energy independent. Therefore it is concluded that the σ_{-0} cross section has anamolous behaviour in Ne target for halogen negative ions and it is in confirmation with the results obtained at low energies.

A comparision with theory could be made only for the Cl^- + Rg system, because the theoretical parameters are not

available for other systems. The predictions of the complex potential theory which had been found to be quite successful in fitting low energy measurements, are far from agreement with the present measurements for the Cl^- + Rg system. The disagreement may be due to the following reasons,

1. The assumptions made in the theoretical model may be suitable at low energies but not at higher energies.
2. The theory does not take into account the excitation occuring either in the projectile or in the target or in both, which may not be important at low energies but may be important in the energy range of the present measurements.

On the other hand the zero radius potential theory gives better agreement with the present measurements for the Cl^- + Ar system, both in magnitude and in the variation with energy. The theory is also found to be good in fitting experimental data[39] for the Br^- + He system. However these agreements may be accidental, since the theory is developed for s-state electrons atomic systems whereas all halogen negative ions have p-state outer electrons.

The measured two electron detachment cross sections have no regular pattern. For the F^- + Rg system, it is of largest magnitude in lighter targets and decreases as the target atomic number increases. In the I^- + Rg system the σ_{-+}^- cross section is target atomic number dependent except in the Ne target where it is smallest. In the Cl^- + Rg system it has an intermediate

behaviour, similar behaviour has been observed[39] for the Br^- + Rg system. The larger magnitude of the σ_+ cross section in lighter targets which have higher ionization potentials, and smaller cross section in heavy targets which have smaller ionization potentials suggests that projectile and the target ionization potentials play an important role in this unusual behaviour which is more evident in the F^- + Rg system and least in the I^- + Rg system. The similarity between the σ_+ and the σ_{0+} cross sections, (which exists only for the F^- + Rg and has not been measured for other systems) suggests that the two electron detachment from a negative ion in a single collision with rare gas atom is a two step processes where the first electron is detached first at some internuclear distance and then the second electron is detached at smaller internuclear separations.

It is concluded from the overal view of the measurements that the single and the two electron detachment cross sections from negative halogen ions in collisions with rare gas atoms, depend on the following factors,

1. The projectile velocity.
2. The projectile and the target atomic numbers.
3. The projectile and the target ionization potentials.

The complications within these factors may arise due to some kind of excitation acompanying the single and the two electron loss processes from negative halogen ions-rare gas collisions. It is

therefore suggested that in order to get more detailed and better information about these processes, more measurements are required especially on the angular distribution of the collision products and on the energy spectra of the ejected electrons during the collision.

REFERENCES

1. J.B.Hasted, Proc. Roy Soc. (London) A 212, 235 (1952).
2. H.S.W.Massey, Negative ions, Cambridge University Press (1937).
3. H.P.Poop, Physics Lett. 16c 169 (1975).
4. B.M.Smirnov, Negative ions, McGraw Hill INc. (1982).
5. Yu.F.Bydin and V.M.Dukelskii, Sov. Phys. JETP 4 474 (1957).
6. S.K.Allison, Rev. Mod. Phys. 30 1137 (1958).
7. J.S.Risley, ICPEAC XIth 619 (1979).
8. J.Fayetoh, D.Dhuicq and M.Barat, J.Phys. B 11 1267 (1978).
9. R.L.Champion and L.D.Doverspike Phys. Rev. A 13 609 (1976).
10. B.T.Smith, W.R.Edwards III, L.D.Doverspike, and R.L. Champion, Phys. Rev. A 18 945 (1978).
11. Yu.N.Demkov, Sov. Phys. JETP 19 762 (1964).
12. A.Z.Devdariani, Sov. Phys. Tech. Phys. 18 255 (1973).
13. Yu.F.Bydin, A.Z.Devdariani and V.V.Kuchinskii Sov. Phys. Tech. Phys. 20 1529 (1976).
14. V.M.Dukelskii and V.V.Fedorenko, Sov. Phys JETP 2 307 (1956).
15. M.Matic and B.Cobic, J.Phys. B 4 111 (1971).
16. B.Hird and F.Rahman, Phys. Rev. A 26 3108 (1982).
17. B.Hird and F.Rahman, Phys. Rev. A 29 1541 (1984).

18. B.Hird and F.Rahman, J.Phys. B 16 3581 (1983).

19. B.Hird and F.Rahman, Can. J.Phys. 62 544 (1984).

20. B.Hird and F.Rahman, (submitted for publication in Phys. Rev. A).

21. R.E.Olson and B.Liu Phys. Rev. A 17 1568 (1978).

22. J.P.Gauyacq, J.Phys. B 12 L387 (1979).

23. J.P.Gauyacq, J.Phys. B 13 L501 (1980).

24. W.J.Lichtenberg, K.Bethge and Schmidt-Bocking J.Phys. B 13 343 (1980).

25. E.A.Mason and J.T.Vanderslice J.Chem. Phys. 28 253 (1958).

26. S.K.Lam, J.B.Delos, R.L.Champion and L.D.Doverspike, Phys. Rev. A 9 1828 (1974).

27. G.P.Lopantseva and O.B.Firsov Sov. Phys. JETP 23 648 (1966).

28. B.Hird and H.C.Suk, Phys. Rev. A 14 928 (1976).

29. V.S.Nikolaev, I.S.Dmtriev, L.N.Fateva and Ya.A.Teplova, Sov. Phys. JETP 13 695 (1961).

30. H.D.Betz, Rev. Mod. Phys. 44 465 (1972).

31. J.Fricke, A.Muller , and E.Salzborn, Nucl. Instrum. Methods 175 379 (1980).

32. M.S.Huq, L.D.Doverspike, R.L.Champion and V.A.Esaulov J.Phys. B 15 951 (1982).

33. C.de.Vreugd, R.W.Wijnaendts Van Resandt and J.Los, Che. Phys. Lett. 65 93 (1979).

34. Ia.M.Fogel, V.A.Ankudinov and D.V.Filipenko Sov. Phys. JETP 19 18 (1960).

35. C.de.Vreugd, R.W.Wijnaendts Van Resandt, J.B.Delos and J.Los, Chem. Phys. 6 261 (1982).

36. S.E.Haywood, D.J.Bowen, R.L.Champion and L.D.Doverspike, J.Phys. B 14 261 (1981).

37. Yu.F.Bydin and A.F.Ioffe, JETP Lett., 6 297 (1967).

38. D.L.Cunningham and A.K.Edwards, Phys. Rev. Lett. 32 915 1974.

39. B.Hird and I.A.Abbas, (to be published).